

The CH fraction of Carbon stars at high Galactic latitudes

Aruna Goswami^{1*}, Drisya Karinkuzhi¹, N S Shantikumar²

¹*Indian Institute of Astrophysics, Koramangala, Bangalore 560034, India*

²*Centre for Research and Education in Science and Technology, Indian Institute of Astrophysics, Shidlaghatta Road, Hosakote 562114, India*

Accepted 2009 October 26. Received 2009, October 26; in original form 2009 September 17

ABSTRACT

CH stars form a distinct class of objects with characteristic properties like iron deficiency, enrichment of carbon and overabundance in heavy elements. These properties can provide strong observational constraints for theoretical computation of nucleosynthesis at low-metallicity. An important question is the relative surface density of CH stars which can provide valuable inputs to our understanding on the role of low to intermediate-mass stars in the early Galactic chemical evolution. Spectroscopic characterization provides an effective way of identifying CH stars. The present analysis is aimed at a quantitative assessment of the fraction of CH stars in a sample of stars using a set of spectral classification criteria. The sample consists of ninety two objects selected from a collection of candidate Faint High Latitude Carbon stars from the Hamburg/ESO survey. Medium resolution ($\lambda/\delta\lambda \sim 1300$) spectra for these objects were obtained using OMR at VBO, Kavalur and HFOSC at HCT, IAO, Hanle, during 2007 - 2009 spanning a wavelength range 3800 - 6800 Å. Spectral analysis shows 36 of the 92 objects to be potential CH stars; combined with our earlier studies (Goswami 2005, Goswami et al. 2007) this implies $\sim 37\%$ (of 243) objects as the CH fraction. We present spectral descriptions of the newly identified CH star candidates. Estimated effective temperatures, $^{12}\text{C}/^{13}\text{C}$ isotopic ratios and their locations on the two colour J-H vs H-K plot are used to support their identification.

Key words: stars: CH stars - variable: carbon - stars: spectral characteristics - stars: AGB - stars: population II

1 INTRODUCTION

Carbon-rich stars ($[\text{C}/\text{Fe}] \geq +1.0$) comprise a significant fraction of metal-poor ($[\text{Fe}/\text{H}] \leq -2.0$) stars with estimates ranging from $14 \pm 4\%$ (Cohen et al. 2005) to $21 \pm 2\%$ (Lucatello et al. 2005); this fraction increases with decreasing metallicity (Rossi, Beers and Sneden 1999). A large fraction of carbon-enhanced metal-poor stars exhibit overabundances of neutron-capture elements relative to iron. Significant insight into the neutron-capture processes taking place in the early Galaxy can be derived from chemical composition studies of metal-poor carbon-stars (Norris et al. 1997a 1997b, 2002; Bonifacio et al. 1998; Hill et al. 2000; Aoki et al. 2002a,b; Goswami et al. 2006, Aoki et al. 2007). However, formation mechanisms of these stars still remain poorly understood. The prime cause of the origin of C-N stars is believed to be the third dredge-up during the AGB evolutionary phase of low to intermediate-mass stars; the origin of C-R stars as well as SC-type stars still remains unclear (Izzard et al. 2007, Zijlstra 2004).

The population II CH stars, characterized by a strong G-band of CH and s-process elements play significant roles in probing the impact of s-process mechanisms in early Galactic chemical evolution. These stars are classified into two distinct types, the Late-type and the Early-type. This classification is based on their $^{12}\text{C}/^{13}\text{C}$ ratios; stars with a large value of $^{12}\text{C}/^{13}\text{C}$ ratio (≥ 100) belong to Late-type, and those with values of $^{12}\text{C}/^{13}\text{C}$ ratio (≤ 10) belong to Early-type. The two groups follow two distinct evolutionary paths. Late-type CH stars are further identified as intrinsic stars that generate s-process elements internally and the early-type CH stars as extrinsic stars; they receive the s-process elements via binary mass transfer. The chemical composition of early-type CH stars, if remains unaltered, would bear signatures of the nucleosynthesis processes operating in the low-metallicity AGB stars. Abundance analysis of such stars can provide observational constraints for theoretical modelling of s-process nucleosynthesis at very low-metallicity revealing the time of influence of this process on early Galactic Chemical Evolution (GCE).

Although new large-aperture telescopes has substantially enhanced the number of target stars for which high

* E-mail: aruna@iiap.res.in

spectral resolution data with high signal-to-noise ratio can be obtained, literature survey shows not many CH stars have been studied in detail so far. A major difficulty is in distinguishing these objects from other types of carbon stars. In particular, Population I C-R, C-N and dwarf carbon stars exhibit remarkably similar spectra with those of carbon giants. It is important to distinguish them from one another and understand the astrophysical implications of each individual class of stellar population. It is with this motivation we have undertaken to identify the CH stellar content as well as different types in a sample of stars presented by Christlieb et al. (2001b). Using low resolution spectral analysis we have classified the stars based on a set of spectral classification criteria. The present work led to the detection of 36 potential CH star candidates among ninety two objects. Combining this result with our previous studies we find $\sim 37\%$ (of 243) objects are potential CH star candidates. This set of objects would make important targets for detailed chemical composition studies based on high resolution spectroscopy.

Selection of the program stars is outlined in section 2. Observations and data reductions are described in section 3. In section 4 we briefly discuss the main features and spectral characteristics of C-stars. Description of the program stars spectra and results are drawn in section 5. Conclusions are presented in section 6.

2 SELECTION OF PROGRAM STARS

The program stars belong to the list of 403 Faint High Latitude Carbon (FHLC) stars presented by Christlieb et al. (2001b) from the database of Hamburg/ESO Survey (HES) described by Wisotzki et al. (2000). Hamburg/ESO Survey for carbon stars covers 6400 degree² limited by $\delta \leq +2.5^0$ and $||b|| \geq 30^0$. The magnitude limit is $V \sim 16.5$. The wavelength range of the spectra is 3200 to 5200 Å at a resolution of 15 Å at H γ . Christlieb et al. found a total of 403 FHLC stars in this survey by application of an automated procedure to the digitized spectra.

The identification of these objects as FHLC stars was based on a measure of line indices - i.e. ratios of the mean photographic densities in the carbon molecular absorption features and the continuum band passes. The primary consideration is the presence of strong C₂ and CN molecular bands shortward of 5200 Å; CH bands were not considered.

At high galactic latitudes different kinds of carbon stars such as N-type carbon stars, dwarf carbon stars, CH-giants, warm C-R stars etc. are known to populate the region (Green et al. 1994). Goswami (2005) and Goswami et al. (2007) have conducted spectral classification of about 151 objects that belong to the FHLC stars sample offered by Christlieb et al. (2001b). These studies are enhanced by medium resolution spectroscopic analysis of an additional sample of ninety two objects observed during 2007 to 2009.

3 OBSERVATIONS AND DATA REDUCTION

Observations were carried out using the 2-m Himalayan Chandra Telescope (HCT) at the Indian Astronomical Observatory (IAO), Mt. Saraswati, Digpa-ratsa Ri, Hanle. The

spectrograph used is the Himalayan Faint Object Spectrograph Camera (HFOSC). HFOSC is an optical imager cum a spectrograph for conducting low and medium resolution grism spectroscopy (<http://www.iap.res.in/centers/iao>). The grism and the camera combination used for observation provided a spectral resolution of $\sim 1330(\lambda/\delta\lambda)$; the observed bandpass ran from about 3800 to 6800 Å. All the objects listed in Table 1 and 2 are observed during 2007 - 2009. The B_J, V, B-V, U-B colours listed in the tables are taken from Christlieb et al. (2001b). Determination of these values are described in Wisotzki et al. (2000) and Christlieb et al. (2001a). B_J magnitudes are accurate to better than ± 0.2 mag including zero point errors (Wisotzki et al. 2000). Spectra of HD 182040, HD 26, HD 5223, HD 209621, Z PSc, V460 Cyg and RV Sct used for comparison were obtained during earlier observations using the same observational set up. A few spectra acquired using the OMR spectrograph at the cassegrain focus of the 2.3-m Vainu Bappu Telescope (VBT) at Kavalur, cover a wavelength range 4000 - 6100 Å at a resolution of ~ 1000 . With a 600 line mm⁻¹ grating, we get a dispersion of 2.6 Å pixel⁻¹.

Observations of Th-Ar hollow cathode lamp taken immediately before and after the stellar exposures provide the wavelength calibration. The CCD data were reduced using the IRAF software spectroscopic reduction packages. For each object two spectra were taken and combined to increase the signal-to-noise ratio.

4 CHARACTERISTICS OF CARBON STARS AND SPECTRAL CLASSIFICATION

Spectral classification helps reducing the number of stars to be analyzed to a tractable number of prototype objects of different groups; each group may be correlated with one or more physical parameters such as luminosity and temperature. Abundance anomalies observed in carbon stars cannot be explained on the basis of observed temperature and luminosity of the stars; it is therefore difficult to devise a classification scheme for carbon stars based on only these two physical parameters. Morgan-Keenan system for carbon star classification (Keenan 1993) divided carbon stars into C-R, C-N and C-H sequence, with subclasses running to C-R6, C-N6 and C-H6 according to temperature criteria. In the old R-N system, CH stars that were classified as R-peculiar are put in a separate class in the new system. In the following we briefly discuss the main characteristics that place carbon stars into different groups. Detailed discussions on carbon stars are available in literature including Wallerstein and Knapp (1998) and references therein.

In contemporary stellar classification schemes assigning stars to 'morphological groups' is largely in practice. Carbon stars are primarily classified based on the strength of carbon molecular bands. The C-N stars are characterized by strong depression of light in the violet part of the spectrum. The cause of rapidly weakening continuum below about 4500 Å is not fully established yet, but believed to be due to scattering by particulate matter. Oxygen-rich stars of similar effective temperatures do not show such weakening. C-N stars are also easily detected for their characteristic infrared colours. The majority of C-N stars show ratios of ¹²C/¹³C in the range of 30 to 100 while in C-R stars this ratio ranges from

Table 1: HE stars with prominent C₂ molecular bands observed during 2007 - 2009

Star No.	RA(2000) ^a	DEC(2000) ^a	<i>l</i>	<i>b</i>	B _J ^a	V ^a	B-V ^a	U-B ^a	J	H	K	Dt of Obs
HE 0008-1712	00 11 19.2	-16 55 34	78.5866	-76.2106	16.5	15.2	1.78	1.64	13.630	13.069	12.975	06.12.2008 11.09.2008
HE 0009-1824	00 12 18.5	-18 07 55	75.8376	-77.2654	16.5	15.7	1.09	0.58	14.080	13.724	13.665	12.09.2008
HE 0037-0654	00 40 02.0	-06 38 13	114.8865	-69.3303	16.4	15.5	1.19	0.58	14.146	13.708	13.724	11.09.2008
HE 0052-0543	00 55 00.0	-05 27 02	125.3316	-68.3057	16.5	15.0	1.95	1.74	12.952	12.241	12.086	12.09.2008
HE 0100-1619	01 02 41.6	-16 03 01	136.7651	-78.6185	15.9	14.7	1.54	1.28	13.114	12.537	12.476	21.11.2008 12.09.2008
HE 0136-1831	01 39 01.8	-18 16 43	176.4932	-75.9157	16.9	15.6	1.72	1.43	14.216	13.679	13.532	12.09.2008
HE 0217+0056	02 20 23.5	+01 10 39	163.6094	-54.5125	16.3	14.6	2.35	2.25	11.276	10.271	9.833	22.11.2008
HE 0225-0546	02 28 19.4	-05 32 58	174.1738	-58.4222	16.5	15.2	1.79	1.51	13.347	12.707	12.528	06.12.2008
HE 0228-0256	02 31 15.5	-02 43 07	171.5942	-55.8545	16.2	14.7	1.99	1.52	12.506	11.813	11.531	18.01.2009
HE 0308-1612	03 10 27.1	-16 00 41	201.1165	-55.9582	12.5	—	—	—	10.027	9.475	9.331	21.11.2008
HE 0420-1037	04 22 47.0	-10 30 26	205.0454	-37.7176	15.2	14.7	1.38	0.99	12.341	11.815	11.695	21.11.2008
HE 0945-0813	09 48 18.7	-08 27 40	245.0790	33.1497	16.2	15.3	1.22	1.11	13.531	13.026	12.903	08.04.2007 09.04.2007
HE 0954+0137	09 57 19.2	+01 23 00	237.1030	41.0018	16.6	15.7	1.18	0.32	—	—	—	21.11.2008
HE 1011-0942	10 14 25.0	-09 57 54	251.7699	36.8590	15.4	14.2	1.65	1.76	11.209	10.432	10.125	22.11.2008
HE 1019-1136	10 22 14.7	-11 51 39	255.1421	36.8087	15.2	13.9	1.84	2.29	10.005	9.031	8.488	06.02.2009
HE 1027-2501	10 29 29.5	-25 17 16	266.6832	27.4163	13.9	12.7	1.73	1.51	10.627	9.896	9.722	22.11.2008
HE 1045-1434	10 47 44.1	-14 50 23	263.5905	38.4049	15.5	14.6	1.23	0.96	12.935	12.449	12.244	09.04.2007
HE 1051-0112	10 53 58.8	-01 28 15	253.5294	49.7900	17.0	16.0	1.44	0.94	14.347	13.794	13.703	06.12.2008
HE 1102-2142	11 04 31.2	-21 58 29	272.5241	34.5071	16.0	14.9	1.44	0.98	13.275	12.714	12.601	16.03.2009
HE 1110-0153	11 13 02.7	-02 09 28	261.1493	52.4883	16.5	15.5	1.47	1.29	12.912	12.205	12.063	04.04.2009
HE 1116-1628	11 19 03.9	-16 44 50	273.2181	40.7347	16.6	15.6	1.28	1.41	13.241	12.614	12.482	06.02.2009
HE 1119-1933	11 21 43.5	-19 49 47	275.7342	38.2583	12.8	14.6	1.34	0.87	13.043	12.571	12.422	18.03.2009
HE 1120-2122	11 23 18.6	-21 38 33	277.1276	36.7743	12.9	—	—	—	9.573	8.902	8.788	17.03.2009
HE 1123-2031	11 26 08.7	-20 48 19	277.4490	37.8097	16.8	15.8	1.33	1.19	13.513	12.940	12.800	18.03.2009
HE 1127-0604	11 29 36.8	-06 20 51	269.3427	51.1090	16.8	15.9	1.23	0.87	14.594	14.087	14.027	18.01.2009
HE 1142-2601	11 44 52.9	-26 18 29	284.8485	34.2157	13.9	13.0	1.28	1.07	11.218	10.675	10.539	04.04.2009
HE 1145-1319	11 48 21.4	-13 36 38	280.3756	46.4800	16.4	15.4	1.37	1.32	13.466	12.934	12.790	17.03.2009 05.04.2009
HE 1146-0151	11 49 02.3	-02 08 11	273.2807	57.0990	14.9	14.2	0.96	0.97	12.929	12.400	12.262	16.03.2009
HE 1157-1434	12 00 11.5	-14 50 50	284.8854	46.2211	16.1	13.8	1.62	1.41	11.792	11.178	11.019	06.06.2007 07.06.2007
HE 1205-0521	12 07 53.	-05 37 51	283.5026	55.5893	15.2	14.4	1.09	0.48	12.434	11.988	11.806	04.04.2009
HE 1205-2539	12 08 08.1	-25 56 38	290.8957	35.9137	13.6	15.4	1.91	1.72	12.313	12.665	12.540	17.03.2009
HE 1210-2636	12 12 59.7	-26 53 22	292.4334	35.1974	13.8	12.6	1.65	1.52	—	—	—	06.05.2009
HE 1228-0417	12 31 12.5	-04 33 40	293.4045	57.9360	14.8	14.0	1.17	0.96	12.406	11.969	11.818	04.04.2009
HE 1230-0327	12 33 24.1	-03 44 28	294.2159	58.8251	13.7	15.1	1.02	0.80	13.683	13.224	13.100	17.03.2009
HE 1238-0836	12 41 02.4	-08 53 06	298.5709	53.8987	13.1	—	—	—	9.189	8.503	8.154	08.04.2007
HE 1253-1859	12 56 38.4	-19 15 32	304.6277	43.5957	13.7	12.9	1.09	1.22	10.604	9.972	9.850	16.03.2009
HE 1315-2035	13 17 57.4	-20 50 53	311.2275	41.5961	16.7	15.7	1.35	0.93	13.678	13.236	13.047	06.05.2009
HE 1331-2558	13 34 20.1	-26 13 38	314.7873	35.6550	13.9	16.0	1.53	1.10	10.998	10.394	10.240	18.03.2009
HE 1344-0411	13 47 25.7	-04 26 04	328.2429	55.6614	16.3	14.9	2.02	2.29	11.708	10.848	10.467	05.04.2009
HE 1358-2508	14 01 12.3	-25 22 39	322.8426	34.4322	13.2	12.3	1.25	0.84	9.521	8.802	8.532	18.01.2009
HE 1400-1113	14 03 39.8	-11 28 04	329.7145	47.6129	16.0	15.2	1.19	0.75	13.838	13.411	13.276	17.03.2009
HE 1404-0846	14 06 55.1	-09 00 58	332.3876	49.4897	15.3	14.2	1.52	1.29	12.435	11.783	11.681	07.06.2007
HE 1405-0346	14 07 58.3	-04 01 03	336.5341	53.7853	14.7	13.5	1.68	1.28	11.608	11.068	10.903	16.03.2009
HE 1410-0125	14 13 24.7	-01 39 54	340.6313	55.0908	—	—	—	—	10.360	9.770	9.651	16.03.2009 11.06.2008
HE 1418-0306	14 20 57.1	-03 19 54	341.7366	52.6618	—	13.0	1.66	1.11	10.505	9.767	9.505	09.04.2007
HE 1425-2052	14 28 39.5	-21 06 05	331.4023	36.3382	13.6	12.7	1.27	1.29	10.043	9.446	9.273	17.03.2009
HE 1428-1950	14 30 59.4	-20 03 42	332.6046	37.0083	—	—	—	—	9.988	9.469	9.318	06.02.2009
HE 1429-1411	14 32 40.6	-14 25 06	336.6322	41.7341	12.5	11.1	1.99	1.89	7.622	6.721	6.346	06.02.2009
HE 1430-0919	14 33 12.9	-09 32 53	340.3560	45.7983	14.9	13.8	1.46	0.75	12.476	11.971	11.862	18.03.2009 09.05.2007
HE 1431-0755	14 34 32.7	-08 08 37	341.8828	46.7820	14.6	13.5	1.51	1.44	11.283	10.605	10.422	08.05.2007
HE 1439-1338	14 42 26.4	-13 51 18	339.7039	40.9588	14.5	13.5	1.39	0.97	10.810	10.112	9.836	25.07.2008 09.04.2007
HE 1440-1511	14 43 07.1	-15 23 48	338.737	39.5765	14.6	13.8	1.13	0.87	12.238	11.757	11.606	09.05.2007
HE 1442-0058	14 44 48.9	-01 10 56	351.4558	50.6883	17.8	16.2	2.15	1.80	12.287	11.268	10.751	06.06.2007
HE 1447+0102	14 50 15.1	+00 50 15	355.2263	51.2262	15.6	15.0	0.90	0.14	13.207	12.760	12.682	12.09.2008 08.04.2007
HE 1525-0516	15 27 52.2	-05 27 04	358.1110	40.1019	16.8	15.8	1.29	1.14	13.972	13.479	13.314	11.09.2008 07.06.2007 08.06.2007
HE 2114-0603	21 17 20.8	-05 50 48	45.5467	-34.9459	16.7	15.4	1.80	1.58	12.472	11.786	11.615	11.09.2008 09.05.2007
HE 2144-1832	21 46 54.7	-18 18 15	34.6476	-46.7834	12.6	—	—	—	—	—	—	06.06.2007
HE 2157-2125	22 00 25.5	-21 11 23	32.0715	-50.7274	16.8	15.9	1.29	1.02	14.389	13.980	13.742	06.06.2007 12.09.2008
HE 2211-0605	22 13 53.5	-05 51 06	55.3066	-46.9505	16.0	15.1	1.21	1.01	13.383	12.875	12.727	24.07.2008
HE 2213-0017	22 15 37.1	-00 02 59	62.3019	-43.8276	16.4	14.6	2.38	2.52	10.860	9.832	9.351	24.07.2008 27.05.2007
HE 2216-0202	22 18 47.5	-01 47 36	61.0859	-45.5370	17.2	16.4	1.01	0.43	14.571	14.165	14.028	06.12.2008 11.09.1008 24.07.2009
HE 2222-2337	22 25 38.8	-23 22 44	31.2015	-56.9371	17.1	15.7	1.93	1.84	13.535	12.837	12.664	12.09.2008
HE 2225-1401	22 28 10.7	-13 46 23	47.4570	-54.0483	16.5	14.5	2.72	2.36	11.870	10.748	9.896	21.11.2008
HE 2228-0137	22 31 26.2	-01 21 42	64.4957	-47.7030	15.8	14.7	1.56	1.20	12.301	11.715	11.589	11.09.2008 25.07.2009
HE 2246-1312	22 49 26.4	-12 56 35	53.2930	-58.1569	17.0	15.9	1.56	1.60	14.101	13.472	13.303	11.09.2008 25.07.2008
HE 2255-1724	22 58 06.8	-17 08 19	47.9045	-62.0030	16.1	15.1	1.45	1.05	12.931	12.374	12.310	11.09.2008 25.07.2008
HE 2305-1427	23 08 10.9	-14 11 27	55.9986	-62.6875	16.4	15.3	1.41	0.80	13.269	12.762	12.744	25.07.2008
HE 2334-1723	23 37 03.7	-17 06 34	59.3241	-70.1108	16.1	15.1	1.38	1.48	13.583	13.119	12.977	10.10.2008 10.10.2008
HE 2347-0658	23 49 56.3	-06 41 55	84.5844	-64.8865	16.9	16.0	1.30	0.69	14.568	14.145	14.158	25.07.2008 11.09.2008
HE 2353-2314	23 55 44.0	-22 58 09	48.1281	-76.7257	16.5	15.2	1.82	1.53	13.064	12.403	12.199	24.07.2008 25.07.2008

^a From Christlieb et al. (2001b)

4 to 9 (Lambert et al. 1986). They have lower temperatures and stronger molecular bands than those of C-R stars. They are used as tracers of an intermediate age population in extragalactic objects.

CH stars are characterised by the strong G-band of CH in their spectra. They form a group of warm stars of equiva-

lent spectral types, G and K normal giants, but show weaker metallic lines. In general, CH stars are high velocity objects, large radial velocities indicating that they belong to the halo population of the Galaxy (McClure 1983, 1984, McClure & Woodsworth 1990). ‘CH-like’ stars, where CH are less dominant have low space velocities (Yamashita 1975). From ra-

Table 2: HE stars without prominent C₂ molecular bands observed during 2007 - 2009

Star No.	RA(2000) ^a	DEC(2000) ^a	<i>l</i>	<i>b</i>	B _J ^a	V ^a	B-V ^a	U-B ^a	J	H	K	mol. bands	Dt of Obs
HE 0422-2518	04 24 38.5	-25 12 10	223.2761	-42.4854	13.9	—	—	—	—	—	—	CH, CN	22.11.2008
HE 0443-2523	04 45 17.7	-25 17 48	224.9946	-38.0024	13.8	—	—	—	10.704	10.169	10.012	CH, CN	06.12.2008
HE 0513-2008	05 15 14.9	-20 04 59	221.6222	-29.8139	13.2	—	—	—	9.398	8.810	8.677	CH, CN	18.01.2009
HE 1027-2644	10 29 57.8	-26 59 51	267.8862	26.0820	14.4	13.4	1.40	1.59	—	—	—	—	17.01.2009
HE 1033-0059	10 36 34.0	+00 43 39	246.4726	48.2458	12.9	13.0	1.10	1.29	10.709	10.138	9.951	CH, CN	09.04.2007
HE 1036-2615	10 38 25.9	-26 30 50	269.3336	27.5445	14.6	13.7	1.21	1.49	—	—	—	CH, CN	17.01.2009
HE 1037-2644	10 40 02.3	-27 00 36	269.9776	27.3253	14.3	13.4	1.33	1.38	—	—	—	CH, CN	06.02.2009
HE 1056-1855	10 59 12.2	-19 11 08	269.4843	36.2931	13.6	—	—	—	10.784	10.249	10.090	CH, CN	22.11.2008
HE 1104-1442	11 06 30.3	-14 58 56	268.5996	40.7912	—	13.7	1.31	1.16	12.217	11.568	11.470	CH, CN	09.04.2007
HE 1105-2736	11 07 44.7	-27 52 35	276.5372	29.6271	14.1	13.2	1.30	1.23	11.314	10.742	10.551	CH, CN	17.03.2009
HE 1112-2557	11 15 14.1	-26 13 28	277.4416	31.8419	14.5	13.6	1.29	1.45	11.548	11.006	10.849	CH, CN	06.05.2009
HE 1150-2546	11 53 15.5	-26 03 41	286.9462	34.9979	15.6	—	—	—	—	—	—	—	18.03.2009
HE 1152-2432	11 54 35.0	-24 48 44	286.8824	36.2813	—	—	—	—	9.413	8.833	8.686	CH, CN	18.03.2009
HE 1229-1857	12 31 46.8	-19 14 02	296.5412	43.3938	14.6	14.0	0.85	0.73	12.124	11.569	11.459	CH, CN	04.04.2009
HE 1236-0036	12 39 25.4	-00 52 58	296.5586	61.8402	16.5	13.5	0.92	0.94	11.679	11.176	11.104	CH, CN	08.05.2007
HE 1406-2016	14 09 44.1	-20 30 57	326.6476	38.7233	15.1	14.2	1.28	1.22	12.092	11.558	11.423	CH, CN	16.03.2009
HE 1420-1659	14 23 03.1	-17 12 51	332.7845	39.8992	13.1	—	—	—	9.871	9.226	9.067	CH, CN	18.01.2009
HE 1514-0207	15 16 38.9	-02 18 33	358.6655	44.2895	13.6	—	—	—	10.335	9.703	9.536	CH, CN	24.07.2008
HE 2115-0709	21 17 42.1	-06 57 11	44.4121	-35.5571	15.1	16.2	1.68	1.70	12.673	12.000	11.808	CH, CN	07.06.2007
HE 2121-0313	21 23 46.2	-03 00 51	49.5147	-34.9016	14.9	13.9	1.35	1.47	11.304	10.718	10.592	CH, CN	11.06.2008
HE 2124-0408	21 27 06.8	-03 55 22	49.0907	-36.0859	14.8	13.9	1.26	1.15	11.578	10.986	10.848	CH, CN	24.07.2008
HE 2205-1033	22 08 29.2	-10 18 37	48.6453	-48.1654	12.8	—	—	—	9.732	9.178	8.980	CH, CN	24.07.2008

^a From Christlieb et al. (2001b)**Table 3: Potential CH star candidates**

Star No.	RA(2000) ^a	DEC(2000) ^a	<i>l</i>	<i>b</i>	B _J ^a	V ^a	B-V ^a	U-B ^a	J	H	K	Dt of Obs
HE 0008-1712	00 11 19.2	-16 55 34	78.5866	-76.2106	16.5	15.2	1.78	1.64	13.630	13.069	12.975	06.12.2008
HE 0052-0543	00 55 00.0	-05 27 02	125.3316	-68.3057	16.5	15.0	1.95	1.74	12.952	12.241	12.086	11.09.2008
HE 0100-1619	01 02 41.6	-16 03 01	136.7651	-78.6185	15.9	14.7	1.54	1.28	13.114	12.537	12.476	12.09.2008
HE 0136-1831	01 39 01.8	-18 16 43	176.4932	-75.9157	16.9	15.6	1.72	1.43	14.216	13.679	13.532	21.11.2008
HE 0225-0546	02 28 19.4	-05 32 58	174.1738	-58.4222	16.5	15.2	1.79	1.51	13.347	12.707	12.528	06.12.2008
HE 0308-1612	03 10 27.1	-16 00 41	201.1165	-55.9582	12.5	—	—	—	10.731	9.821	9.406	21.11.2008
HE 0420-1037	04 22 47.0	-10 30 26	205.0454	-37.7176	15.2	14.7	1.38	0.99	12.341	11.815	11.695	21.11.2008
HE 1027-2501	10 29 29.5	-25 17 16	266.6832	27.4163	13.9	12.7	1.73	1.51	10.627	9.896	9.722	22.11.2008
HE 1045-1434	10 47 44.1	-14 50 23	263.5905	38.4049	15.5	14.6	1.23	0.96	12.935	12.449	12.244	09.04.2007
HE 1051-0112	10 53 58.8	-01 28 15	253.5294	49.7900	17.0	16.0	1.44	0.94	14.347	13.794	13.703	06.12.2008
HE 1102-2142	11 04 31.2	-21 58 29	272.5241	34.5071	16.0	14.9	1.44	0.98	13.275	12.714	12.601	16.03.2009
HE 1110-0153	11 13 02.7	-02 09 28	261.1493	52.4883	16.5	15.5	1.47	1.29	12.912	12.205	12.063	04.04.2009
HE 1119-1933	11 21 43.5	-19 49 47	275.7342	38.2583	12.8	14.6	1.34	0.87	13.043	12.571	12.422	18.03.2009
HE 1120-2122	11 23 18.6	-21 38 33	277.1276	36.7743	12.9	—	—	—	9.573	8.902	8.788	17.03.2009
HE 1123-2031	11 26 08.7	-20 48 19	277.4490	37.8097	16.8	15.8	1.33	1.19	13.513	12.940	12.800	18.03.2009
HE 1142-2601	11 44 52.9	-26 18 29	284.8485	34.2157	13.9	13.0	1.28	1.07	11.218	10.675	10.539	04.04.2009
HE 1145-1319	11 48 21.4	-13 36 38	280.3756	46.4800	16.4	15.4	1.37	1.32	13.466	12.934	12.790	17.03.2009
HE 1146-0151	11 49 02.3	-02 08 11	273.2807	57.0990	14.9	14.2	0.96	0.97	12.929	12.400	12.262	05.04.2009
HE 1157-1434	12 00 11.5	-14 50 50	284.8854	46.2211	16.1	13.8	1.62	1.41	11.792	11.178	11.019	16.03.2009
HE 1205-2539	12 08 08.1	-25 56 38	290.8957	35.9137	13.6	15.4	1.91	1.72	13.313	12.665	12.540	06.06.2007
HE 1210-2636	12 12 59.7	-26 53 22	292.4334	35.1974	13.8	12.6	1.65	1.52	—	—	—	07.06.2007
HE 1228-0417	12 31 12.5	-04 33 40	293.4045	57.9360	14.8	14.0	1.17	0.96	12.406	11.969	11.818	17.03.2009
HE 1253-1859	12 56 38.4	-19 15 32	304.6277	43.5957	13.7	12.9	1.09	1.22	10.60	9.972	9.850	06.05.2009
HE 1331-2558	13 34 20.1	-26 13 38	314.7873	35.6550	13.9	16.0	1.53	1.10	10.998	10.394	10.240	04.04.2009
HE 1404-0846	14 06 55.1	-09 00 58	332.3876	49.4897	15.3	14.2	1.52	1.29	12.435	11.783	11.681	18.03.2009
HE 1405-0346	14 07 58.3	-04 01 03	336.5341	53.7853	14.7	13.5	1.68	1.28	11.608	11.068	10.903	07.06.2007
HE 1410-0125	14 13 24.7	-01 39 54	340.6313	55.0908	—	—	—	—	10.360	9.770	9.651	16.03.2009
HE 1425-2052	14 28 39.5	-21 06 05	331.4023	36.3382	13.6	12.7	1.27	1.29	10.043	9.446	9.273	11.06.2008
HE 1431-0755	14 34 32.7	-08 08 37	341.8828	46.7820	14.6	13.5	1.51	1.44	11.283	10.605	10.422	17.03.2009
HE 1440-1511	14 43 07.1	-15 23 48	338.737	39.5765	14.5	13.5	1.13	0.87	12.238	11.757	11.606	08.05.2007
HE 1447+0102	14 50 15.1	+00 50 15	355.2263	51.2262	15.6	15.0	0.90	0.14	13.207	12.760	12.682	09.05.2007
HE 1525-0516	15 27 52.2	-05 27 04	358.1110	40.1019	16.8	15.8	1.29	1.14	13.972	13.479	13.314	08.04.2007
HE 2114-0603	21 17 20.8	-05 50 48	45.5467	-34.9459	16.7	15.4	1.80	1.58	12.472	11.786	11.615	11.06.2008
HE 2211-0605	22 13 53.5	-05 51 06	55.3066	-46.9505	16.0	15.1	1.21	1.01	13.383	12.875	12.727	07.06.2007
HE 2228-0137	22 31 26.2	-01 21 42	64.4957	-47.7030	15.8	14.7	1.56	1.20	12.301	11.715	11.589	08.06.2007
HE 2246-1312	22 49 26.4	-12 56 35	53.2930	-58.1569	17.0	15.9	1.56	1.60	14.101	13.472	13.303	11.09.2008

^a From Christlieb et al. (2001b)

dial velocity survey CH stars are known to be binaries. According to the models of McClure (1983, 1984) and McClure & Woodsworth (1990) the CH binaries have orbital characteristics consistent with the presence of a white dwarf companion. Early type CH stars are believed to have conserved the products of the carbon rich primary received through mass transfer and survived until the present in the Galactic halo. CH stars are not a homogeneous group of stars. They consist of two populations, the most metal-poor ones have a spherical distribution and the ones slightly richer in metals are characterised by a flattened ellipsoidal distribution (Zinn 1985). The ratio of the local density of CH stars was

found to be $\sim 30\%$ of metal-poor giants (Hartwick & Cowley 1985).

Many C-R stars also show a quite strong G band of CH in their spectra. Hence, based only on the strength of the G-band of CH it is not possible to make a distinction between CH and C-R stars. In such cases the secondary P-branch head near 4342 Å serves as a more useful indicator. This is a well-defined feature in CH stars spectra in contrast to its appearance in C-R stars spectra (refer Fig 2, 3 of Goswami 2005). Another important diagnostic feature is Ca I at 4226 Å which in case of CH stars is weakened by the overlying CH band systems. In C-R star's spectra this feature is quite strong; usually the line depth is deeper than the depth of the

CN molecular band around 4215 Å. These spectral characteristics allow for an identification of the CH and C-R stars even at low resolution.

Abundances of neutron-capture elements can also be used as an useful indicator of spectral type. The abundances of s-process elements are nearly solar in C-R stars (Dominy 1984); whereas the CH stars show significantly enhanced abundances of the s-process elements relative to iron (Lambert et al. 1986, Green and Margon 1994). Although, the C-R as well as CH stars have warmer temperatures than those of C-N stars and blue/violet light is accessible to observation and atmospheric analysis, at low dispersion the narrow lines are difficult to estimate and elemental abundances can not be determined. At low dispersion, therefore, the ‘abundance criteria’ can not be used to distinguish the C-R stars from the CH stars. Although the CH and C-R stars have similar range of temperatures, the distribution of CH stars place most of them in the Galactic halo. The large radial velocities, typically $\sim 200 \text{ km s}^{-1}$ of the CH stars are indicative of their being halo objects (McClure 1983, 1984).

C-J stars spectra are characterized by strong Merrill-Sanford (M-S) bands ascribed to SiC_2 that appear in the wavelength region 4900 - 4977 Å. The SiC_2 being a triatomic molecule, M-S bands are expected to be the strongest in the coolest stars. SiC_2 and C_3 have similar molecular structures and in many C stars C_3 molecule is believed to be the cause of ultraviolet depression (Lambert et al. 1986). These bands are absent in the spectra of known CH stars. A few warmer C-N stars are known to exhibit the presence of M-S bands in their spectra. Strength of M-S bands are known to show a distinct correlation with carbon isotopic ratios; i.e., stars with higher $^{12}\text{C}/^{13}\text{C}$ ratios show weaker M-S bands. WZ Cas, V Aql & U Cam are a few exceptions that have low ^{13}C and strong M-S bands (Barnbaum et al. 1996). Strong C-molecular bands but a weak CH band characterize the class of hydrogen deficient carbon stars.

We have classified the program stars guided by the above spectral characteristics. In the present sample of ninety two stars the spectra of twenty two objects are found to not exhibit molecular bands of C_2 . These objects are listed in Table 2. Among the seventy stars that exhibit strong carbon molecular bands (Table 1) thirty six of them are found to show spectral characteristics of CH stars. These potential CH star candidates are listed in Table 3. In the following we discuss the spectral characteristics of the individual objects.

5 RESULTS AND DISCUSSIONS

The spectra of the objects are primarily examined in terms of the following spectral characteristics.

1. The strength (band depth) of the CH band around 4300 Å.
2. Prominence of the secondary P-branch head near 4342 Å.
3. Strength/weakness of the Ca I feature at 4226 Å.
4. Isotopic band depths of C_2 and CN, in particular the Swan bands of $^{12}\text{C}^{13}\text{C}$ and $^{13}\text{C}^{13}\text{C}$ near 4700 Å.
5. Strengths of the other C_2 bands in the 6000 -6200 Å region.
6. The ^{13}CN band near 6360 Å and the other CN bands

across the wavelength range.

7. Presence/absence of the Merrill-Sanford bands around 4900 - 4977 Å region.

8. Strength of the Ba II features at 4554 Å and 6496 Å.

The membership of a star in a particular group is established from a differential analysis of the program stars spectra with the spectra of the comparison stars. Spectra of carbon stars available in the low resolution spectral atlas of carbon stars of Barnbaum et al. (1996) are also consulted. In Figure 1 we reproduce the spectra of the comparison stars in the wavelength region 4000 - 6800 Å; in figure 2 we show one example of HE stars spectra from the present sample corresponding to each comparison star’s spectrum in figure 1.

5.1 Location of the candidate CH stars on (J-H) vs (H-K) plot

We have used JHK photometry as supplementary diagnostics for stellar classification. Figure 3 shows the locations of the candidate CH stars listed in Table 3 on the (J-H) vs (H-K) plot. 2MASS JHK measurements of the stars are available on-line at <http://www.ipac.caltech.edu/>. The thick box on the lower left represents the location of CH stars and the thin box on the upper right represents the location of C-N stars (Totten et al. 2000). Except two lying outside (shown with open squares in figure 3), the locations of the candidate CH stars (shown with open circles) are well within the CH box. This supports their identification with the class of CH stars. Location of the comparison CH stars HD 26, HD 5223 and HD 209621, C-R star RV Sct, C-N stars V460 Cyg and Z PSc, are shown by solid squares on the (J-H) vs (H-K) plot. As described in the next section, we have also used 2MASS JHK photometry to determine the effective temperatures of the objects.

5.2 Effective temperatures of the program stars

Semiempirical temperature calibrations offered by Alonso et al. (1994, 1996, 1998) are used to derive preliminary temperature estimates of the program stars. These authors used the infrared flux method to measure temperatures for a large number of lower main sequence stars and subgiants to derive the calibrations. The calibrations relate T_{eff} with Stromgren indices as well as $[\text{Fe}/\text{H}]$ and colours (V-B), (V-K), (J-H) and (J-K). The calibrations hold within a temperature and metallicity range $4000 \leq T_{\text{eff}} \leq 7000 \text{ K}$ and $-2.5 \leq [\text{Fe}/\text{H}] \leq 0$. The estimated uncertainty in T_{eff} arising from different sources is $\sim 90 \text{ K}$ (Alonso et al. 1996). Alonso et al. derived the T_{eff} scales using photometric data measured on TCS system; 2MASS JHK photometric data are therefore converted to the TCS system using the conversion relations of Ramirez and Melendez (2004). Estimation of T_{eff} from (J-H) & (V-K) temperature relations involve a metallicity term; (J-K) calibration relation is independent of metallicity. We have estimated the effective temperatures using adopted metallicities shown in parenthesis in Table 4. (B-V) calibration, normally used in case of normal stars is not considered as in the case of carbon stars the colour B-V depends on the chemical composition and metallicity

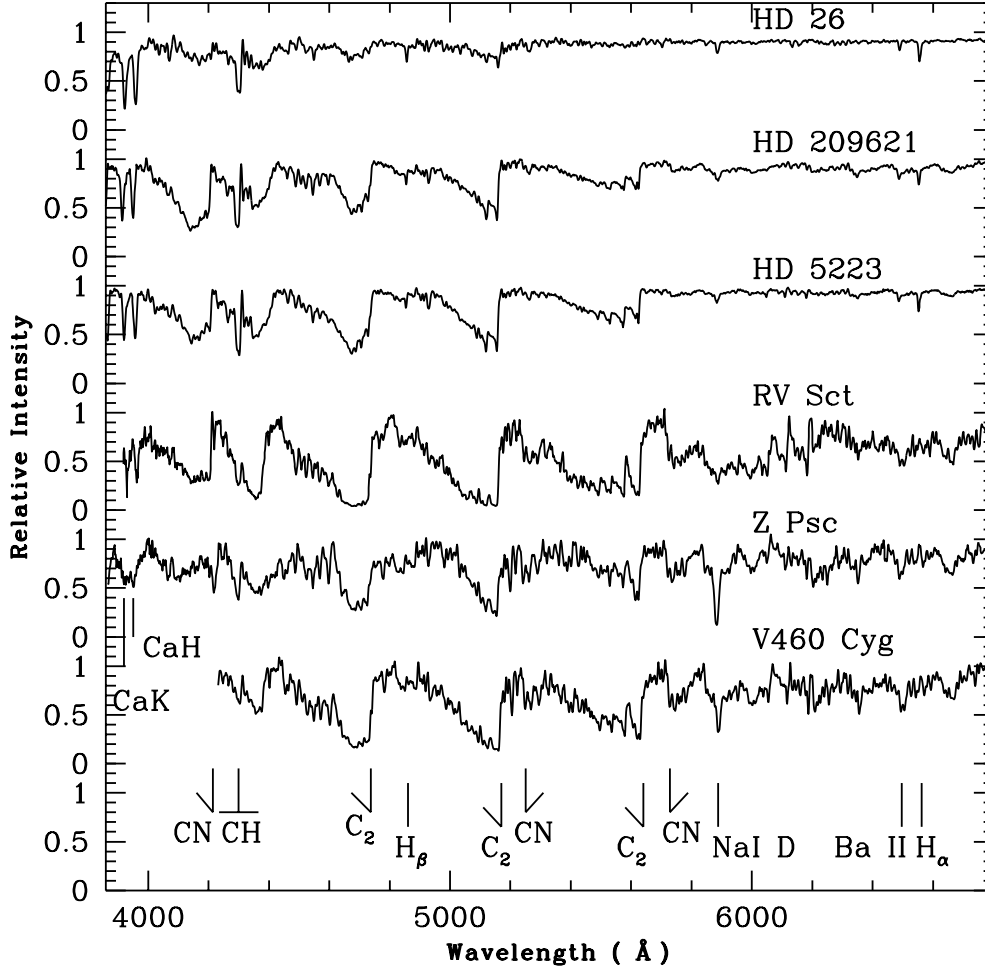


Figure 1. The spectra of the comparison stars in the wavelength region 3860 - 6800 Å. Prominent features seen on the spectra are indicated.

in addition to T_{eff} . B-V colour often gives a much lower value than the actual surface temperature of the star due to the effect of CH molecular absorption in the B band. We have assumed that the effects of reddening on the measured colours are negligible.

5.3 Isotopic ratio $^{12}\text{C}/^{13}\text{C}$ from molecular band depths

Carbon isotopic ratios $^{12}\text{C}/^{13}\text{C}$, widely used as mixing diagnostics provide an important probe of stellar evolution. These ratios measured on low resolution spectra do not give accurate results but provide a fair indication of evolutionary states of the objects.

We have estimated these ratios, whenever possible, using the molecular band depths of (1,0) $^{12}\text{C}^{12}\text{C}$ $\lambda 4737$ and (1,0) $^{12}\text{C}^{13}\text{C}$ $\lambda 4744$. For a majority of the candidate CH stars, the ratios $^{12}\text{C}/^{13}\text{C}$ are found to be ≤ 10 . These ratios for HD 26, HD 5223 and HD 209621 are respectively 5.9, 6.1 and 8.8 (Goswami 2005).

Our estimated ratios of $^{12}\text{C}/^{13}\text{C}$ indicate that most of

the candidate CH stars belong to the ‘early-type’ category. The low carbon isotope ratios imply that, in a binary system, the material transferred from the now unseen companion has been mixed into the CN burning region of the CH stars or constitute a minor fraction of the envelope mass of the CH stars. Low isotopic ratios are typical of stars on their first ascent of the giant branch. The $^{12}\text{C}/^{13}\text{C}$ ratios and the total carbon abundances decrease due to the convection which dredges up the products of internal CNO cycle to stellar atmosphere as ascending RGB. If it reaches AGB stage, fresh ^{12}C may be supplied from the internal He burning layer to stellar surface leading to an increase of $^{12}\text{C}/^{13}\text{C}$ ratios again.

5.4 Spectral characteristics of the candidate CH stars

HE 0420-1037, 1102-2142, 1142-2601, 1146-0151, 1210-2636, 1253-1859, 1447+0102. The spectra of these objects resemble closely the spectrum of HD 26. HD 26 is a known classical CH star with effective temperature 5170 K and $\log g = 2.2$ (Vantures 1992b). The temperatures

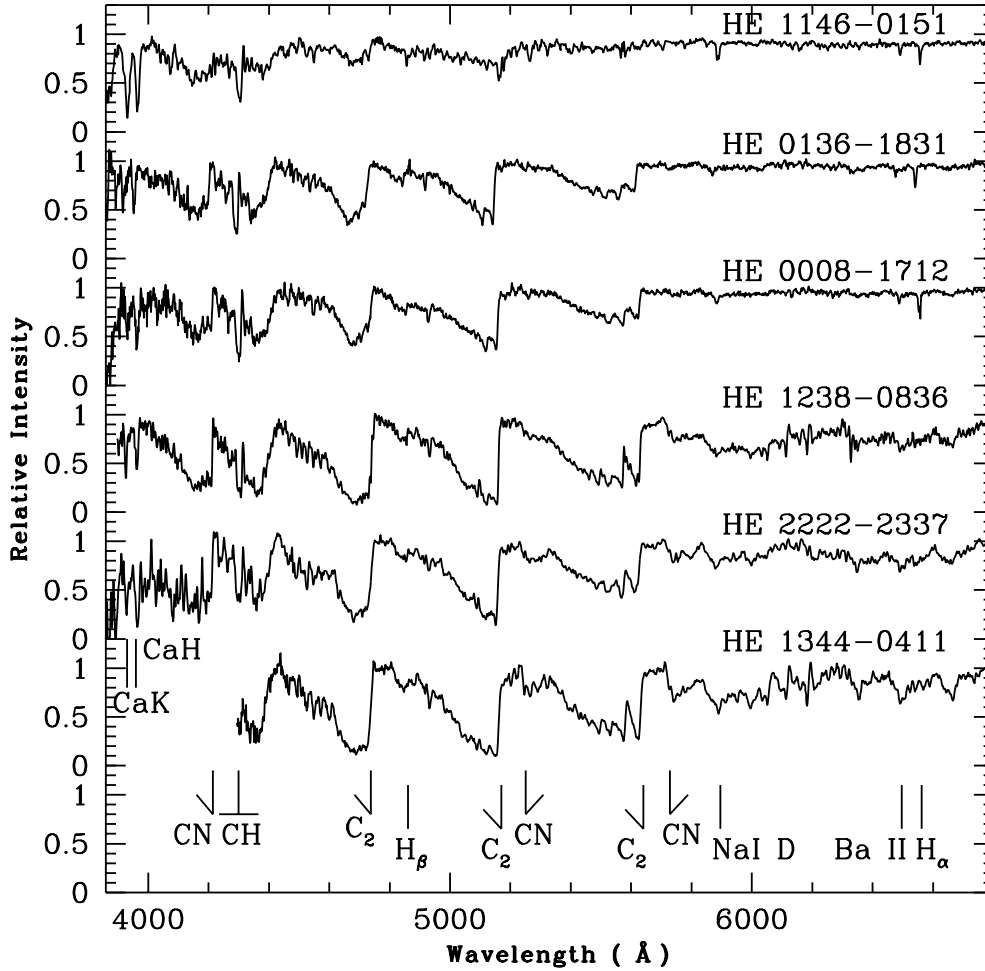


Figure 2. An example of each of the HE stars corresponding to the comparison stars presented in Figure 1, in the top to bottom sequence, in the wavelength region 3860 - 6800 Å. The locations of the prominent features seen in the spectra are marked on the figure.

of these objects as measured using JHK photometric data range from 4200 to 5000 K. The locations of these objects are well within the CH box in figure 3. In figure 4, we show as an example, a comparison of the spectra of three objects HE 0420-1037, HE 1142-2601 and HE 1146-0151 with the spectrum of HD 26. With marginal differences in the strengths of the molecular features, the spectra of these three objects show more or less a good match with their counterparts in HD 26. The CN band around 4215 Å and the C₂ band around 5165 Å in the spectra of HE 0420-1037 and HE 1146-0151 are marginally stronger; the Na I D feature also appears stronger. The features due to Ca K and H appear with similar strengths. In the spectrum of HE 1142-2601, the CN band depth around 4215 Å and Ca II K and H line depths are deeper than their counterparts in HD 26. The Ca I line at 4226 Å is detected with line depth weaker than the band depth around 4215 Å. In HD 26, the Ca I 4226 Å feature is not detected. The object HE 1253-1859 also have very similar spectrum with that of HD 26. The CN band around 4215 Å and carbon isotopic band around 4730 Å are stronger, but the CH band, Ca II

K and H features are of similar strengths. The molecular bands around 5165 Å and 5635 Å show an exact match. The lines due to Na I D, Ba II at 6496 Å and H_α are seen equally strongly as in HD 26. The Ca I feature at 4226 Å could not be detected and the secondary P-branch head around 4342 Å seems to be marginally weaker. In the spectrum of HE 1102-2142 the molecular C₂ bands around 4735, 5165 and 5635 Å are slightly deeper than those in HD 26. The CN band around 4215 Å and the CH band around 4310 Å also appear marginally stronger in the spectrum of HE 1102-2142. The H_α feature and the Ba II line at 6496 Å are marginally weaker; the feature due to Na I D appears with similar strength as in HD 26. H_β at 4861 Å is clearly seen. The Ca I line at 4226 Å is weakly detected. In the spectrum of HE 1210-2636, the CN band around 4215 Å and the secondary P-branch head around 4342 Å appear slightly stronger than in HD 26. The C₂ molecular band around 5165 Å is also slightly weaker. The carbon isotopic band around 4733 Å is marginally detectable. Ca I line at 4226 Å could not be detected. Features due to Ca II K and H and H_α are clearly detected. In the spectrum

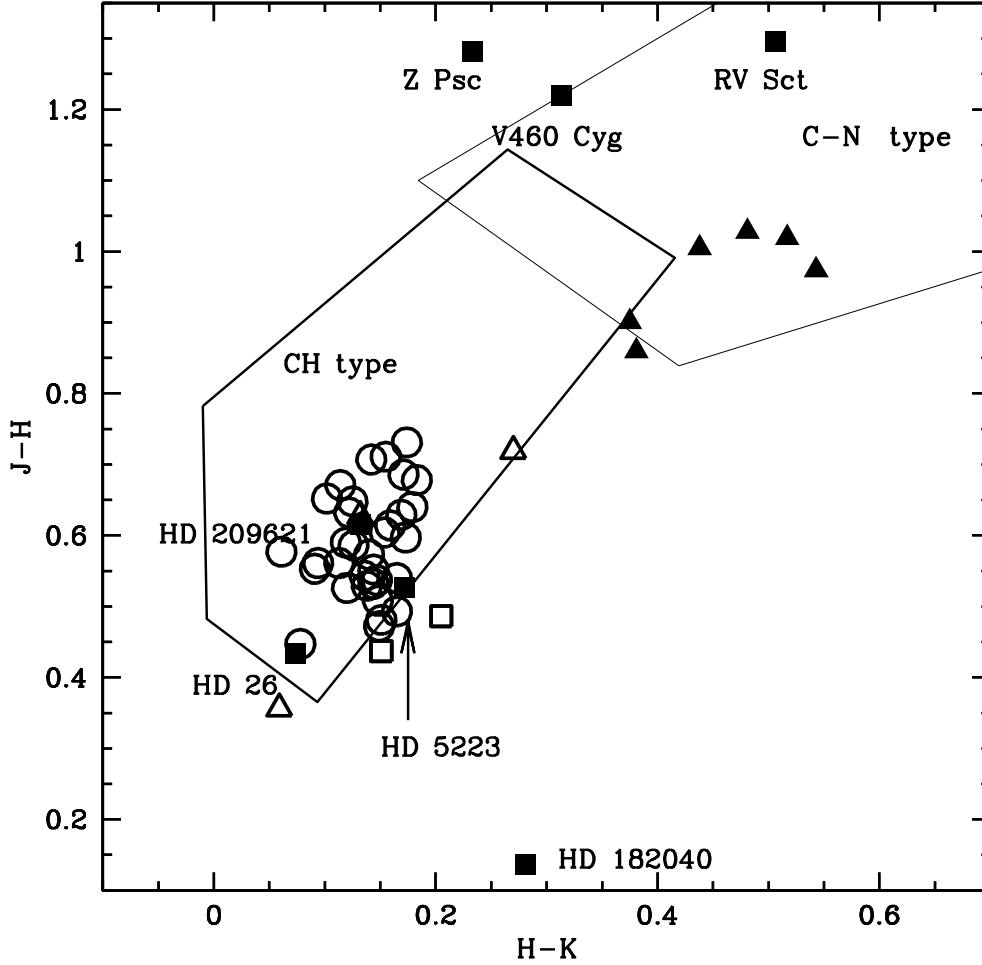


Figure 3. A two colour J-H versus H-K diagram of the candidate CH stars. The thick box on the lower left represents the location of CH stars and the thin box on the upper right represents the location of C-N stars (Totten et al. 2000). Majority of the candidate CH stars listed in Table 3 (represented by open circles) fall well within the CH box. The positions of the two outliers are shown with open squares. C-N stars found in our sample are represented by solid triangles. The location of the comparison stars are labeled and marked with solid squares. Location of the three dwarf carbon stars are indicated by open triangles.

of HE 1447+0102, the CN band around 4215 Å is almost absent. Strong well defined features due to Ca II K and H are seen. Molecular bands around 4733, 5165, and 5635 Å are distinctly seen to be stronger than their counterparts in HD 26. In the redward of 5700 Å no molecular bands are detected. We assign these objects to the CH group.

HE 0136-1831, 0308-1612, 1027-2501, 1051-0112, 1119-1933, 1120-2122, 1123-2031, 1145-1319, 1205-2539, 1331-2558, 1404-0846, 1425-2052, 1525-0516, 2114-0603, 2211-0605, 2228-0137, 2246-1312. The spectra of these objects resemble closely the spectrum of HD 209621, a classical CH star with effective temperature ~ 4400 K (Tsuji et al. 1991). The effective temperatures estimated for this set of objects using JHK photometry range from 3948 K (HE 2114-0603) to 4675 K (HE 1119-1933). Their locations on the J-H vs H-K plot are well within the CH box in figure 3. Three exam-

ples, HE 0136-1831, HE 1027-2501 and HE 2228-0137 from this set are shown in figure 5 together with the spectrum of HD 209621. In the spectrum of HE 0136-1831, the CN band around 4215 Å is marginally weaker and the carbon molecular bands around 4733 and 5635 Å are marginally stronger than those in HD 209621. All other features show a good match. The spectrum of HE 1027-2501 also shows a close match with the spectrum of HD 209621. Except for the molecular bands around 4733, 5165 and 5635 Å that appear marginally weaker in the spectrum of HE 2228-0137 the spectrum of this object bears a close resemblance with the spectrum of HD 209621. The spectrum of HE 0308-1612 shows weaker molecular bands around 5165 Å and 5635 Å. The CN band around 4215 Å and the carbon isotopic band around 4730 Å are of similar strengths. The CH band around 4300 Å and Ca II K and H features are of similar depths. The lines due to Na I D, Ba II at 6496 Å and H_α are clearly noticed. The Ca I feature at 4226 Å could not

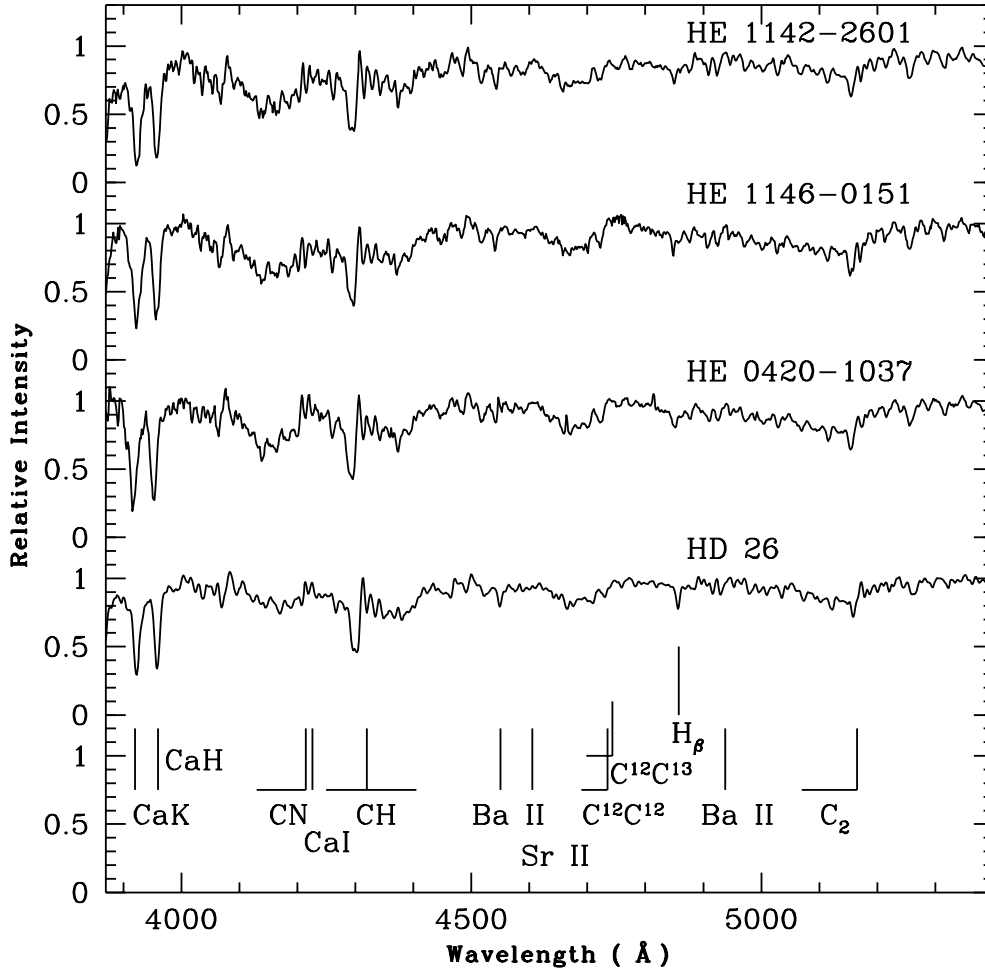


Figure 4. A comparison of the spectra of three HE stars in the wavelength region 3870 - 5400 Å with the spectrum of the comparison star HD 26. Prominent features noticed in the spectra are marked on the figure.

be detected. The spectrum of HE 1051-0112 shows a weaker CN band around 4215 Å. The G-band of CH appears with almost the same strength as in HD 209621. The secondary P-branch head around 4342 Å and the bands around 4730 and 5635 Å are relatively stronger. Features due to Ca II K and H are barely detectable in the spectrum of this object. The molecular band around 5165 Å shows an exact match with its counterpart in HD 209621. The features due to H α and Na I D are detected distinctly; the Ba II feature at 6496 Å is marginally detected.

In the spectrum of HE 1119-1933, Ca II K and H appear marginally stronger. The molecular band around 5365 Å appears marginally weaker than in HD 209621. The spectra of HE 1120-2122 and HE 1123-2031 are very similar, both exhibit a weaker CN band around 4215 Å. All other features show a good match with their counterparts in the spectrum of HD 209621. Ca II K and H appear with almost the same strength in the spectrum of HE 1120-2122 as in HD 209621. Ca I line at 4226 Å is not detectable. The spectra of HE 1123-2031, HE 1145-1319, HE 1205-2539, HE 1331-2558 are noisy shortward of 4100 Å and the lines

due to Ca II K and H could not be clearly detected. Ca I line at 4226 Å is not detectable in these spectra. Features due to Na I D, H α , and Ba II at 6496 Å are detected. In the spectrum of HE 1145-1319, C₂ molecular bands around 5635 and 4733 Å are marginally deeper than those in HD 209621. The features redward of 4200 Å in the spectrum of HE 1205-2539 show a good match with those in HD 209621. The molecular features in the spectrum of HE 1331-2558 are also of similar strengths with those in HD 209621. Except for the G-band of CH, all other molecular features are weaker in the spectrum of HE 1404-0846. The features due to Ca II K and H are marginally stronger. The spectrum of HE 1404-0846 is noisy at the blue end.

In the spectrum of HE 1425-2052 the G-band of CH and the C₂ band around 5635 Å are mildly stronger. The rest of the features show a close match with their counterparts in HD 209621. The Ba II feature at 6496 Å appears with equal intensity as that of H α feature. The feature due to Na I D is clearly detected. In the spectrum of HE 1525-0516, H α and Na I D features are detected with almost equal strength as in HD 209621. The spectrum of

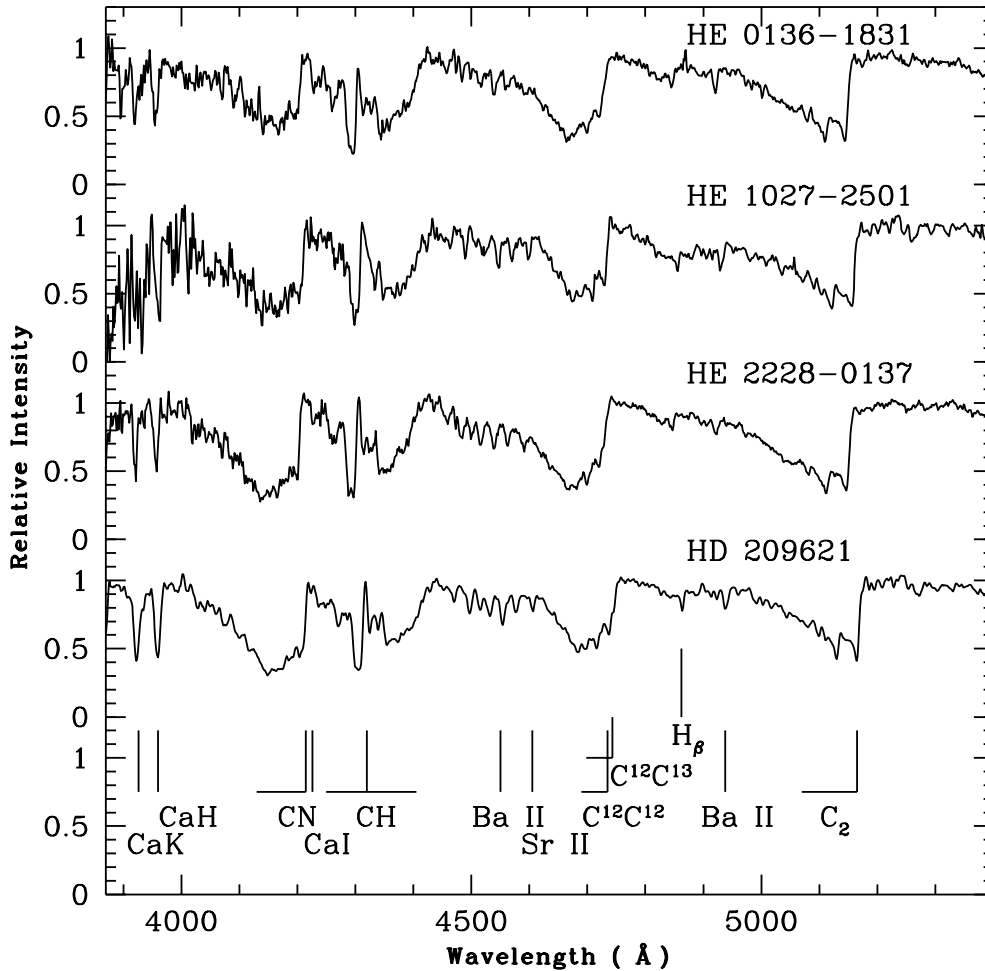


Figure 5. A comparison of the spectra of three HE stars in the wavelength region 3870 - 5400 Å with the spectrum of the comparison star HD 209621. Prominent features noticed in the spectra are marked on the figure.

HE 2114-0603 shows a remarkably close match with the features in HD 209621 including those longward of 5700 Å. However the features due to Ca II K and H that are seen very distinctly in the spectrum of HD 209621 could not be detected in the spectrum of HE 2114-0603; the spectrum is noisy blueward of 4000 Å. In the spectrum of HE 2211-0605 the molecular features are weaker than their counterparts in HD 209621 but stronger than those in HD 26. The CH band matches exactly with the one in HD 209621. Ca II K and H appear with almost equal strengths as in HD 209621. The spectrum of HE 2246-1312 shows a weaker molecular band around CN 4215 Å. Other molecular bands appear with almost of equal strengths as their counterparts in HD 209621. The spectrum blueward of 4100 Å is noisy and Ca II K and H features could not be detected as well defined features. The spectrum obtained in september 2008 has a better signal.

HE 0008-1712, 0052-0543, 0100-1619, 0225-0546, 1045-1434, 1110-0153, 1157-1434, 1228-0417, 1405-0346, 1410-0125, 1431-0755, 1440-1511. The

spectra of these objects closely resemble the spectrum of HD 5223, a well-known classical CH star with effective temperature ~ 4500 K, $\log g = 1.0$ and metallicity $[\text{Fe}/\text{H}] = -2.06$ (Goswami et al. 2006). The effective temperatures of these objects derived from J-K colour range from about 3924 K (HE 0052-0543) to 4795 K (HE 1228-0417). Except for the two outliers HE 1045-1434 and HE 1228-0417 (represented with open squares) the locations of this set of objects are well within the CH box in figure 3.

A comparison of the spectra of HE 0008-1712, HE 0100-1619 and HE 1405-0346 with the spectrum of HD 5223 is shown in figure 6. The Ca I line at 4226 Å is not detectable in any of these spectra. The CH band as well as other molecular bands show a very good match. The features due to Ca II K and H are seen with equal strength as in HD 5223. The CN band around 4215 Å in HE 0100-1619 is slightly deeper. The bands longward of 5635 Å are also marginally deeper. This object HE 0100-1619 is also mentioned as a CH star in Totten et al. (2000). Heliocentric radial velocity of HE 0100-1619 as reported by Bothun et al. (1991) is -142 km s^{-1} .

The spectra of HE 0052-0543 and HE 1110-0153

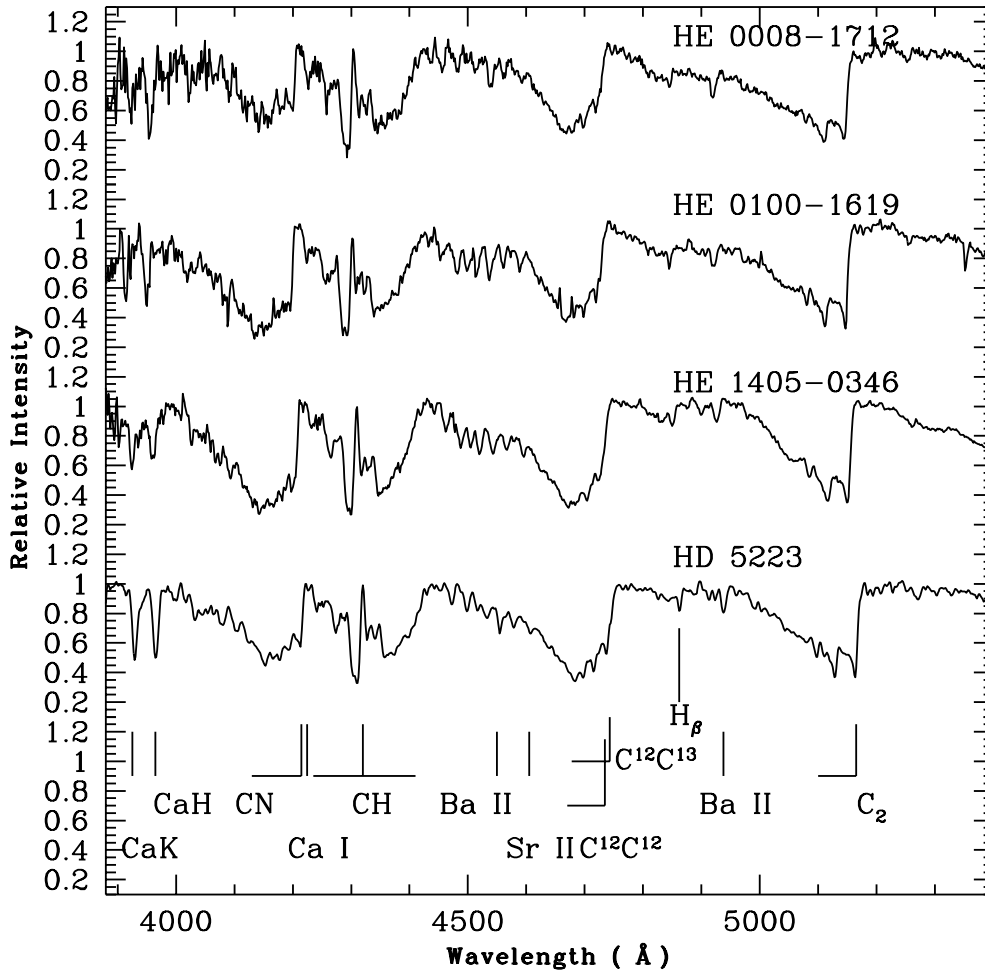


Figure 6. A comparison of the spectra of three HE stars in the wavelength region 3880 - 5400 Å with the spectrum of the comparison star HD 5223. Prominent features noticed in the spectra are marked on the figure.

show stronger molecular bands than their counterparts in HD 5223. In the spectrum of HE 0225-0546 the molecular bands are marginally stronger than in HD 5223. The molecular features above 5700 Å seen in these two spectra are barely noticed in the spectrum of HD 5223. The spectrum of HE 1157-1434 also show a good match with the spectrum of HD 5223 except for the molecular band around 5635 Å which is distinctly weaker in its spectrum. The molecular features redward of 5700 Å are also noticed weakly in the spectrum of this object. The spectrum of HE 1405-0346 shows a stronger CN band around 4215 Å as well as a stronger carbon molecular band around 5635 Å. The secondary P-branch head near 4342 Å is also stronger than its counterpart in HD 5223. Other molecular bands around 4733 and 5165 Å show a good match. Ca II K and H are seen as strongly as in HD 5223. The effective temperature of the object from J-K colour is 4391 K, slightly lower than the effective temperature of HD 5223. In the spectrum of HE 1410-0125 the molecular features are slightly shallower than their counterparts in HD 5223. The CH band depth is however of similar strength. The feature at Ca I 4226 Å

is absent; the features due to Ca II K and H are of similar strengths. The CN band around 4215 Å matches well with the CN feature in HD 5223. The radial velocity of this object as quoted by Frebel et al. (2006) is +80 Km s⁻¹. The effective temperature estimated using (J-K) calibration returns a value 4378 K for this object.

The spectrum of HE 1431-0755 is noisy blueward of 4000 Å; the features of Ca II K and H could not be detected. The CH band around 4310 Å and the CN band around 4215 Å appear slightly stronger than their counterparts in HD 5223. Other C₂ molecular bands present in the spectrum are narrower than their counterparts in HD 5223. The spectrum redward of 5700 Å shows molecular features that are barely noticed in the spectrum of HD 5223. The spectrum of HE 1440-1511 shows molecular bands with almost equal depths with those in HD 5223. Ca II K and H features are however stronger than their counterparts in HD 5223. The spectrum shows a distinctly stronger feature due to Na I D. Features of H_α and Ba II at 6496 Å are of equal strengths. The spectrum redward of 5700 Å shows a good match.

In the spectrum of HE 1228-0417 the Ba II feature at

6496 Å and H α are seen with equal strengths as in HD 5223. The part of the spectrum redward of 5700 Å shows a very good match. The Ca I line at 4226 Å is not detected. The feature due to Na I D is clearly detected. Other carbon molecular features around 4730, 5165, and 5635 Å appear marginally weaker than their counterparts in HD 5223. The G-band of CH appears with almost equal strength but the CN band around 4215 Å is marginally weaker than its counterpart in HD 5223. The effective temperature of the object estimated using J-K colour calibration is 4795 K, higher than the effective temperature of HD 5223 \sim 4500 K (Goswami et al. 2006). The location of this object outside the CH box is not obvious from its low resolution spectra.

HE 0009-1824, 1116-1628, 1358-2508. The spectra of these objects are illustrated in figure 7. These three objects are known dwarf carbon stars. The effective temperatures of HE 0009-1824, HE 1116-1628, HE 1358-2508 as estimated from (J-K) calibration are respectively 5530 K, 4224 K and 3623 K. As expected, the molecular band depths are the strongest in HE 1358-2508, the coolest of the three objects; and weakest in HE 0009-1824. In the spectrum of HE 0009-1824 the CN band around 4215 Å is completely missing. The features due to Ca II K and H as well as the CN band near 3880 Å are detected. The G-band of CH is strong but not as strong as it appears in CH stars. The secondary P-branch head near 4342 Å is seen distinctly. Apart from the absence of the CN band around 4215 Å the spectrum of this object looks somewhat similar to the spectrum of HD 209621. The distance of this object as reported by Maun et al. (2007) is 300 pc.

The spectra of HE 1116-1628 and HE 1358-2508 show characteristics of C-R star RV Sct with marginal differences in the molecular band depths. In the spectrum of HE 1358-2508, the CH band is marginally stronger than in RV Sct. The C₂ molecular bands are stronger in the spectrum of this object. The CN band around 4215 Å is clearly detected. Ratnatunga (1983) first proposed this object HE 1116-1628 to be a dwarf carbon star. This object is also present in the list of dwarf carbon stars of Lowrance et al. (2003). Maun et al. (2007) reported the proper motions in α and δ and their respective 1σ errors in mas yr⁻¹ as -23.5 ± 6.7 and $+29.8 \pm 4.6$. The distances of HE 1116-1628 and HE 1358-2508 as reported by Maun et al. (2007) are 170 pc and 270 pc respectively. Totten and Irwin (1998) reported a radial velocity of -69 km s⁻¹ for the object HE 1116-1628. All the three objects have total proper motion $\mu \geq 30$ mas yr⁻¹ (Maun et al. 2007).

The locations of the three dwarf carbon stars are indicated by open triangles in figure 3. Location of HE 0009-1824 is on the left below the CH box, the location of HE 1358-2508 is on the right edge of the CH box and the location of HE 1116-1628 is found to be well inside the CH box. Dwarf carbon stars have anomalous infrared colours (Green et al. 1992 and Westerlund et al. 1995). In the conventional two colour JHK diagram the locus of dwarf-carbon-stars colours is away from the normal carbon-star locus. The locus defined by dwarf carbon stars is bounded by (J-H) ≤ 0.75 and (H-K) ≥ 0.25 (Westerlund et al. 1995). This condition is satisfied by HE 1358-2508; however HE 0009-1824, and HE 1116-1628 both have (H-K) colours less than the lower limit of 0.25 mag set for dwarf

carbon stars.

Candidate C-N stars: HE 0217+0056, 0228-0256, 1019-1136, 1344-0411, 1429-1411, 1442-0058, 2213-0017, 2225-1401.

The spectra of these objects show a close resemblance with the spectrum of the C-N star Z Psc with similar strengths of CN and C₂ molecular bands across the wavelength regions. In figure 3, the objects HE 0217+0056, HE 1019-1136, HE 1344-0411, HE 1429-1411, HE 1442-0058 and HE 2213-0017 represented by solid triangles lie well within the CN box. The spectra have low flux below about 4400 Å. The spectrum of HE 1429-1411 is similar to that of Z Psc's spectrum, except that the CN band around 4215 Å is marginally weaker in this star. The CH band is weakly detected in the spectrum of HE 1116-1628. The molecular bands near 4735, 5135 and 5635 Å are noticed distinctly. The feature due to Na I D is strongly detectable. The Ba II line at 6496 Å is detectable but the H α feature could not be detected. HE 1127-0604 has low flux below about 4200 Å. The CH band and C₂ molecular bands around 4735, 5165, 5635 Å are detected. All the features in the spectrum are weaker than their counterparts in Z Psc. While features of Ca II K and H are detected, the CN band around 4215 Å is not clearly seen. The spectrum of HE 2225-1401 has low flux below about 4700 Å. The strong C₂ molecular bands around 5165, 5635 Å appear stronger than their counterparts in Z Psc. The spectrum of HE 2225-1401 although have spectral characteristics of C-N stars, its location in figure 3 is not within the CN box. The spectra of the objects HE 2213-0017, HE 1442-0058, HE 1344-0411 compare closest to the spectrum of C-N star V460 Cyg as illustrated in figure 8.

The objects HE 0217+0056, HE 1019-1136, HE 1442-0058, HE 2213-0017 and HE 2225-1401 are also mentioned as N-type stars in the APM survey of cool carbon stars in the Galactic halo (Totten & Irwin 1998). Totten et al. (2000) have provided proper motion measurements for these objects. The distances measured by these authors assuming an average $M_R = -3.5$ for these objects are respectively 24, 16, 43, 29 and 24 kpc. Heliocentric radial velocities estimated by Totten & Irwin (1998) for these objects are respectively -142 ± 3 , 126 ± 4 , 37 ± 4 , -44 ± 3 , and -113 ± 5 km s⁻¹. Heliocentric radial velocity of HE 0228-0256 is -72 km s⁻¹ (Bothun et al. 1991).

HE 0945-0813, 1011-0942, 1127-0604, 1205-0521, 1238-0836, 1418-0306, 1428-1950, 1439-1338, 2222-2337. The spectra of these objects show characteristics of C-R stars. The spectra of HE 1011-0942, HE 1205-0521, HE 1238-0836 match closest to the spectrum of RV Sct. The effective temperatures of the objects estimated using (J-K) calibration range from 3521 K (HE 1238-0836) to 4875 K (HE 1127-0604).

In the spectra of HE 1238-0836 and HE 1428-1950 the CH band around 4300 Å is slightly deeper than in RV Sct. The molecular features in the redward of 5700 Å appear marginally weaker. In the spectra of HE 0945-0813, the CN band around 4215 Å is distinctly detected. Ca I line at 4226 Å which is generally very weak or absent in CH stars appears very strongly in the spectrum of this object. The feature due to Na I D appears very strong. Feature due to the secondary P-branch head around 4342 Å is somewhat

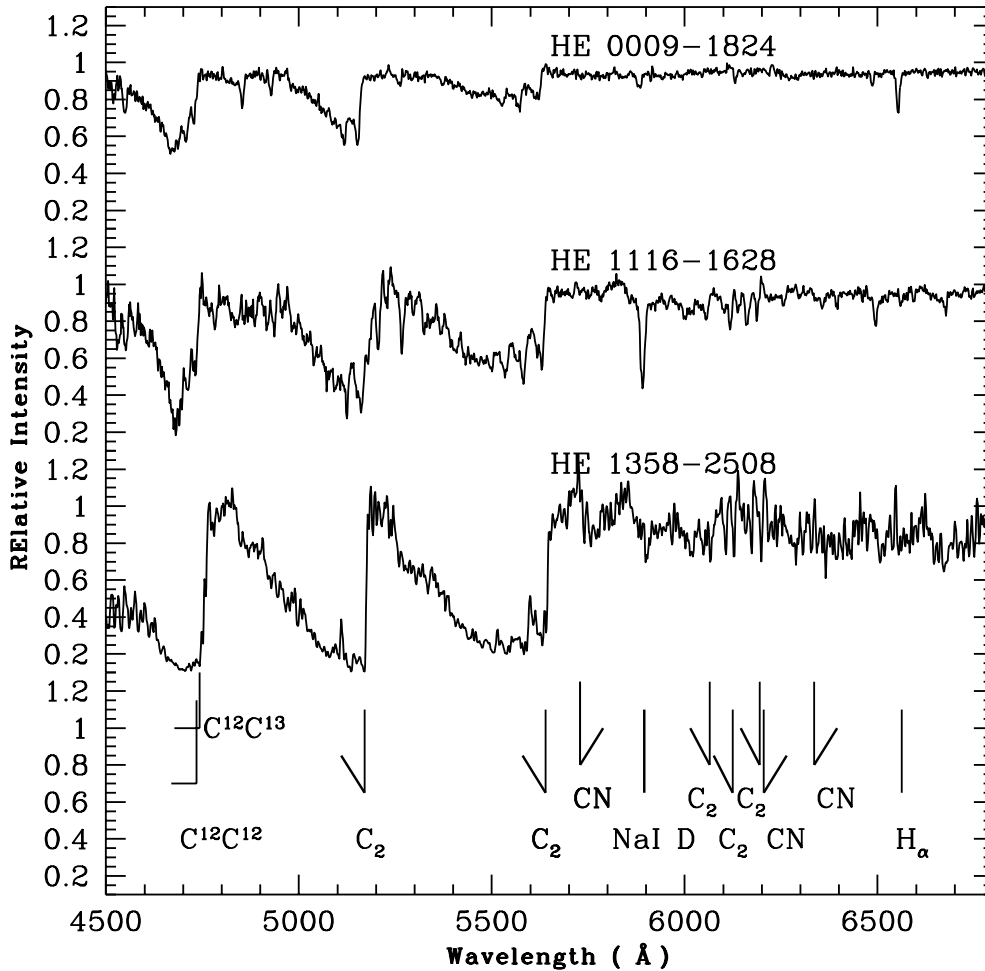


Figure 7. The spectra of three dwarf carbon stars in the wavelength region 4500 - 6800 Å. Prominent features noticed in the spectra are marked on the figure.

noticeable in the spectrum of HE 0945-0813. The lines due to Ba II at 6496 Å and H_α are detected in both the spectra. The molecular bands around 4733, 5165 and 5635 Å appear strongly in the spectrum of HE 0945-0813. The spectrum of HE 2222-2337 has low flux below about 4100 Å. The CH band does not appear as strong as it should be in C-R star's spectrum. The CN band around 4215 Å is marginally detected. Other molecular bands are of similar strengths. The molecular features redward of 5635 Å are slightly weaker. We place these objects in the C-R group.

HE 0037-0654, 0954+0137, 1230-0327, 1400-1113, 1430-0919, 1447-0102, 2157-2125, 2216-0202, 2255-1724, 2305-1427, 2334-1723, 2347-0658, 2353-2314. The spectra of these objects are characterized by a weak (or absent) CN band around 4215 Å. Apart from this feature the spectra are somewhat similar to the spectrum of HD 209621.

The spectrum of HE 1230-0327 shows a strong G-band of CH and a distinct secondary P-branch head near 4342 Å. Ca I feature at 4226 Å is not detected. The CN band

around 4215 Å is almost absent. While atomic lines of Ca II K, H, H_α , Na I D are distinctly seen, Ba II line at 6496 Å is marginally detected. The spectra of HE 0954+0137, HE 1400-1113, HE 1430-0919, HE 2255-1724 and HE 2347-0658 look very similar to the spectrum of HE 1230-0327. In the spectra of these objects the feature due to the CN band around 4215 Å is marginally detectable. Weak molecular bands noticed in the spectrum of HD 209621 upward of 5700 Å are not observable in these spectra. Compared to HD 209621, the molecular bands around 4733, 5165, and 5635 Å are slightly weaker in the spectra of these objects. Ca II K and H are detected almost with equal strength as in HD 209621. In the spectrum of HE 1430-0919 the secondary P-branch head near 4342 Å is marginally weaker than in HD 209621. While the molecular band around 5165 Å shows a good match, the bands around 4733 and 5635 Å are marginally stronger. The spectrum in the redward of 5700 Å resembles the spectrum of HD 209621. Features due to Na I D, H_α and Ba II line at 6496 Å are detected. In the spectrum of HE 1447+0102, the CN band around 4215 Å is almost absent. Strong well defined features of Ca II K and H

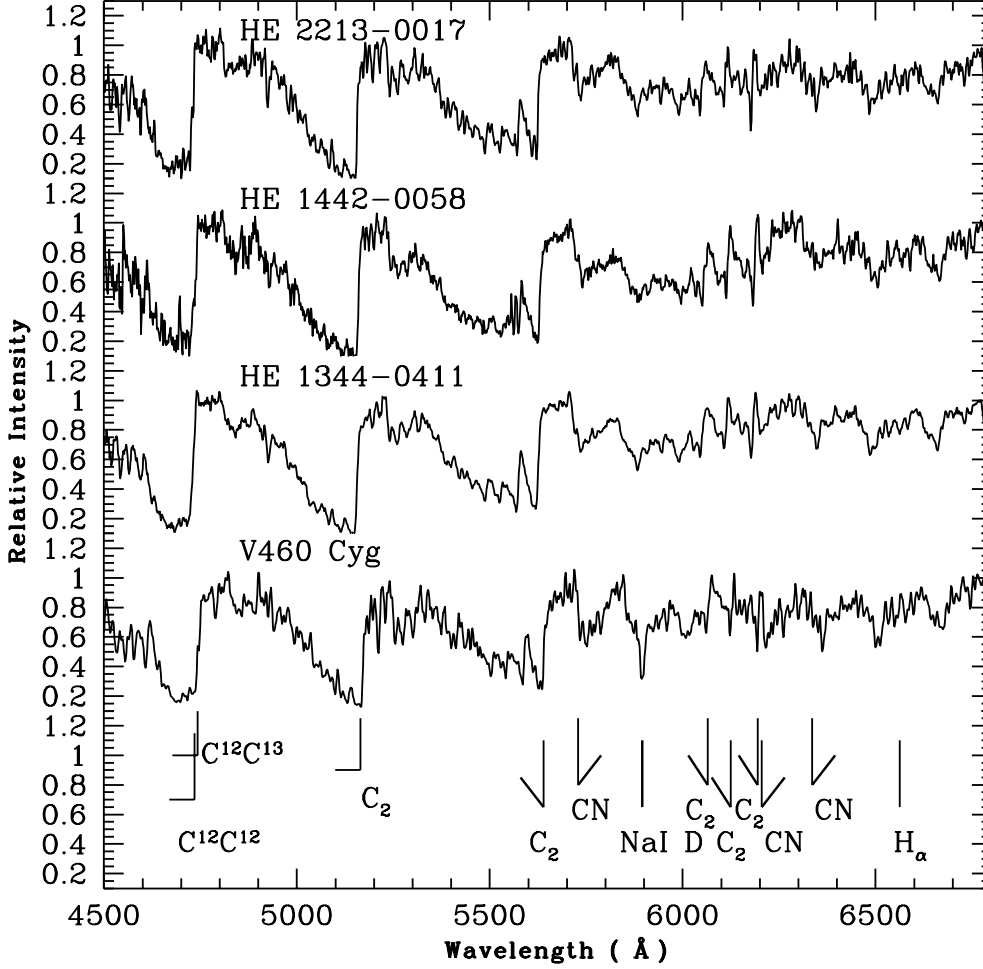


Figure 8. A comparison of the spectra of the candidate C-N stars with the spectrum of V460 Cyg in the wavelength region 4500 - 6800 Å. The bandheads of the prominent molecular bands, Na I D and H α are marked on the figure.

are seen. The C₂ molecular bands around 4733, 5165, 5635 Å are distinctly present. No other molecular bands are noticed longward of 5700 Å. The spectra of HE 2305-1427 and HE 2334-1723 show the CN band around 4215 Å with band depth almost half of that in HD 209621. All other molecular features match well with their counterparts in the spectrum of HD 209621. Weak molecular bands that are noticed in the spectrum of HD 209621 upward of 5700 Å are not noticeable in the spectra of these two objects. The features due to Na I D, H α and Ba II at 6496 Å could be detected. The secondary P-branch head at 4223 Å is seen as distinctly as in HD 209621.

In the spectrum of HE 2353-2314, the CH band around 4300 Å as well as the CN band around 4215 Å are marginally detected. The carbon molecular band around 5165 Å is clearly detected; the band around 5635 Å is much weaker. No other molecular bands or atomic lines are detectable. In the spectrum of HE 2255-1724, the CN band around 4215 Å is much weaker than that in HD 209621. The CH band and Ca II K and H are of similar depths. The molecular bands around 4733, 5165, 5635 Å are slightly

weaker in this object. Features of Na I D, Ba II line at 6496 Å, and H α are distinctly seen. The molecular bands longward of 5635 Å are not detectable. The spectrum acquired on Sep 11, 2008 have a better signal. In the spectrum of HE 2334-1723, the CN band around 4215 Å is much weaker than in HD 209621; all other molecular bands show a good match. The features due to Ca II K and H also show a good match. No molecular bands are detectable upward of 5700 Å. In the spectrum of HE 2347-0658 the CN band around 4215 Å is almost absent. Ca II K and H features and carbon molecular bands around 4733, 5165, 5635 Å show a good match. Molecular bands seen in HD 209621 upward of 5700 Å are not detectable in the spectrum of this object.

The spectrum of HE 1400-1113 is noisy below about 4220 Å. The CN band around 4215 Å could be marginally detected. Ca II K and H are detected as weak features. A strong CH band around 4300 Å and the secondary P-branch head near 4342 Å are distinctly seen. Other molecular features have band depths marginally weaker than their counterparts in HD 209621. Except for Na I D, Ba II at 6496 Å

and H_α no other atomic lines are detected redward of 5670 Å.

The spectrum of HE 1430-0919 also shows a very weak CN band around 4215 Å. The features due to Ca II K and H are not detected. The G-band of CH around 4300 Å is however very strong in the spectrum. The spectrum of HE 2157-2125 shows the CH band around 4300 Å with almost equal strength to its counterpart in HD 209621. Features due to Ca II K and H and other molecular features are also seen with equal intensities. However, the CN band around 4215 Å is much weaker than that in HD 209621. The spectrum obtained in October, 2008 has a better signal than the spectra obtained in June and September, 2008.

The spectrum of HE 0037-0654 looks very similar to the spectrum of HD 26; however, molecular bands of C_2 around 4730, 5165 and 5635 Å are marginally stronger than their counterparts in HD 26. The CN band around 4215 Å is barely detected, much weaker than in HD 26. Ba II line at 6496 Å is clearly detected. Strong lines of H_α and Na I D are distinctly noticed. Except for the features of Ca II K and H which are much weaker, the spectrum of HE 2216-0202 is very similar to the spectrum of HD 26. The secondary P-branch head around 4342 Å is much stronger than in HD 26. The CN band around 4215 Å is not observed. The CH band at 4305 Å is not as strong as in HD 26. The molecular bands around 4733 Å and 5236 Å are of similar depths. The carbon molecular band around 5635 Å is weaker than the band around 5165 Å. No molecular bands longward of 5700 Å are detectable.

The spectrum of HE 1315-2035 is noisy blueward of 4200 Å. The G-band of CH and the carbon molecular bands near 4733, 5165 and 5635 Å are detected in the spectrum. The H_α feature is clearly detected. The effective temperature of this object is 4639 K as estimated from (J-K) colour calibration.

HE 1027-2644. The spectra of HE 1027-2644 do not show presence of any carbon molecular bands. The features due to Ca II K and H are not detected. The G-band of CH is seen as a weak feature. Features due to Ca I at 4226 Å and Na D I are seen as strong features. Ba II line at 6496 Å and H_α feature are detected. 2MASS JHK photometry is not available for this object.

6 CONCLUDING REMARKS

An accurate assessment of the fraction of CH stars can significantly aid our understanding of formation and evolution of heavy elements at low metallicity. Another important issue is the role of low to intermediate-mass stars of the halo in the early Galactic chemical evolution. Thus large samples of faint high latitude stars such as the one reported by Christlieb et al. (2001b) that contain different types of carbon stars need to be analyzed to understand the astrophysical implications of each individual type of stellar population. Our objective in this study has been to identify the CH stars (as well as different type of stellar objects) in a selected sample of high Galactic latitude field stars. The sample is based on our on-going observational programs with HCT and VBT on cool stars. During 2007 and 2009 we have acquired low resolution spectra for a large number of stars

Table 4: Estimated effective temperatures (T_{eff}) from semi-empirical relations

Star Name	Teff(J-K)	Teff(J-H)
HE0008-1712	4556.52	4378.94(-0.5) 4446.43(-2.5)
HE0009-1824	5530.27	5377.40(-0.5) 5443.08(-2.5)
HE0037-0654	5496.71	4912.74(-0.5) 4980.33(-2.5)
HE0052-0543	3924.82	3831.70(-0.5) 3896.64(-2.5)
HE0100-1619	4615.21	4305.94(-0.5) 4373.23(-2.5)
HE0113+0110	4130.72	3973.94(-0.5) 4039.78(-2.5)
HE0136-1831	4459.39	4493.10(-0.5) 4560.81(-2.5)
HE0217+0056	2794.61	3053.31(-0.5) 3110.53(-2.5)
HE0225-0546	4051.67	4086.82(-0.5) 4153.25(-2.5)
HE0228-0256	3655.89	3916.80(-0.5) 3982.30(-2.5)
HE0308-1612	4420.27	4428.17(-0.5) 4495.77(-2.5)
HE0341-0314	4119.26	4336.67(-0.5) 4404.05(-2.5)
HE0420-1037	4587.42	4534.65(-0.5) 4602.42(-2.5)
HE0945-0813	4650.36	4629.30(-0.5) 4697.14 (-2.5)
HE1011-0942	3417.52	3646.15(-0.5) 3709.67(-2.5)
HE1019-1136	2690.13	3140.84(-0.5) 3199.16(-2.5)
HE1028-2501	3824.73	3769.05(-0.5) 3833.54(-2.5)
HE1045-1434	4436.49	4738.21(-0.5) 4806.03(-2.5)
HE1051-0112	4594.34	4411.69(-0.5) 4479.26(-2.5)
HE1102-2142	4492.46	4383.27(-0.5) 4450.77(-2.5)

Table 4: Estimated effective temperatures (T_{eff}) from semi-empirical relations (continued)

Star Name	Teff(J-K)	Teff(J-H)
HE1110-0153	3969.89	3842.74(-0.5) 3907.75(-2.5)
HE1116-1628	4224.43	4125.85(-0.5) 4192.46(-2.5)
HE1119-1933	4675.25	4790.28(-0.5) 4858.06(-2.5)
HE1120-2122	4148.01	3961.57(-0.5) 4027.33 (-2.5)
HE1123-2031	4365.87	4339.85(-0.5) 4407.24(-2.5)
HE1127-0604	4875.50	4604.60(-0.5) 4672.42(-2.5)
HE1142-2601	4475.87	4464.64(-0.5) 4532.31(-2.5)
HE1145-1319	4485.81	4514.13(-0.5) 4581.87(-2.5)
HE1146-0151	4515.88	4525.81(-0.5) 4593.57(-2.5)
HE1157-1434	4182.97	4181.08(-0.5) 4247.93(-2.5)
HE1205-0521	4650.36	4927.12(-0.5) 4994.67(-2.5)
HE1205-2539	4182.97	4046.42(-0.5) 4112.64(-2.5)
HE1228-0417	4795.85	4964.09(-0.5) 5031.55(-2.5)
HE1230-0327	4814.61	4846.74(-0.5) 4914.44(-2.5)
HE1238-0836	3521.23	3954.13(-0.5) 4019.85(-2.5)
HE1253-1859	4239.41	4105.00(-0.5) 4171.51(-2.5)
HE1315-2035	4639.76	4949.26(-0.5) 5016.77(-2.5)
HE1318-1657	4423.50	4612.48(-0.5) 4680.31(-2.5)
HE1331-2558	4227.41	4218.84(-0.5) 4285.84(-2.5)
HE1344-0411	3118.34	3414.55(-0.5) 3475.93(-2.5)

Table 4: Estimated effective temperatures (T_{eff}) from semi-empirical relations (continued)

Star Name	Teff(J-K)	Teff(J-H)
HE1358-2508	3623.67	3826.04(-0.5) 3890.93(-2.5)
HE1400-1113	4894.81	5010.94(-0.5) 5078.27(-2.5)
HE1404-0846	4239.40	4027.25(-0.5) 4093.38(-2.5)
HE1405-0346	4391.32	4484.40(-0.5) 4552.09(-2.5)
HE1410-0125	4378.56	4266.53(-0.5) 4333.70(-2.5)
HE1418-0306	3598.71	3761.98(-0.5) 3826.41(-2.5)
HE1425-2052	4191.80	4250.49(-0.5) 4317.60 (-2.5)
HE1428-1950	4505.82	4573.18 (-0.5) 4640.98(-2.5)
HE1429-1411	3057.76	3302.55(-0.5) 3362.74(-2.5)
HE1430-0919	4700.38	4625.80(-0.5) 4693.64(-2.5)
HE1431-0755	3937.98	3950.23(-0.5) 4015.92(-2.5)
HE1432-2138	5074.94	5075.25(-0.5) 5142.38(-2.5)
HE1439-1338	3658.21	3898.38(-0.5) 3963.76(-2.5)
HE1440-1511	4636.24	4747.85(-0.5) 4815.66 (-2.5)
HE1442-0346	4622.20	4655.40(-0.5) 4723.24(-2.5)
HE1447+0102	5042.06	4893.55 (-0.5) 4961.18(-2.5)
HE1525-0516	4546.30	4695.10 (-0.5) 4762.94(-2.5)
HE2114-0603	3948.56	3919.97(-0.5) 3985.48(-2.5)
HE2157-2125	4583.97	5135.81(-0.5) 5202.71(-2.5)
HE2211-0605	4553.10	4621.90(-0.5) 4689.73(-2.5)

Table 4: Estimated effective temperatures (T_{eff}) from semi-empirical relations (continued)

Star Name	Teff(J-K)	Teff(J-H)
HE2213-0017	2701.10	3005.84(-0.5) 3062.45(-2.5)
HE2216-0202	4969.45	5122.15(-0.5) 5189.11(-2.5)
HE2222-2337	3911.73	3879.01(-0.5) 3944.26(-2.5)
HE2225-1401	2169.18	2845.70(-0.5) 2900.11(-2.5)
HE2228-0137	4369.03	4284.06(-0.5) 4351.28(-2.5)
HE2246-1312	4110.70	4125.95(-0.5) 4192.57(-2.5)
HE2255-1724	4675.26	4388.73(-0.5) 4456.25(-2.5)
HE2305-1427	5042.06	4594.23(-0.5) 4662.05(-2.5)
HE2334-1723	4729.39	4827.13 (-0.5) 4894.87(-2.5)
HE2347-0658	5554.46	4989.70(-0.5) 5057.10(-2.5)
HE2353-2314	3927.44	4014.92(-0.5) 4080.98(-2.5)

The numbers inside the parentheses indicate the adopted metallicities [Fe/H]

Table 5: Stars with radial velocity estimates

Star Name	v_r km s $^{-1}$	Reference
HE 0100-1629	-142.0	1
HE 0217+0056	-142.0 \pm 3	2
HE 0228-0256	-72.0	1
HE 1019-1136	-126.0 \pm 4	2
HE 1105-2736	-36.0 \pm 1.3	3
HE 1116-1628	-69.0	2
HE 1152-0355	+431.3 \pm 1.5	4
HE 1305+0007	+217.8 \pm 1.5	4
HE 1410-0125	+88.0 \pm 3	5
HE 1429-1411	-90.0 \pm 1.5	6
HE 1442-0058	-37.0 \pm 4	2
HE 2213-0017	-44.0 \pm 3	2
HE 2225-1401	-113.0 \pm 5	2
HD 26	+217.8 \pm 1.5	6
HD 5223	-244.9 \pm 1.5	4
HD 209621	-390.5 \pm 1.5	6

References: 1: Bothun et al. (1991), 2: Totten & Irwin (1998), 3: Zwitter et al. (2008), 4: Goswami et al. (2006), 5: Frebel et al. (2006), 6: Goswami et al. (in preparation)

that included about ninety two objects from the Hamburg survey of Christlieb et al. (2001b).

The spectral classification criteria are those presented in Goswami (2005). Among the ninety two objects, the spectra of seventy objects are characterized by the presence of strong C₂ molecular bands. The spectra of twenty two objects show only a weak or moderate G-band of CH and a CN band around 4215 Å. One object, HE 1027-2644 does not show presence of any molecular bands in its spectrum. The spectral analysis led to the detection of thirty six potential CH star candidates. Their locations on the two color J-H versus H-K diagram, estimated effective temperatures, and carbon isotopic ratios are in support of their classification with this class of objects. This set of objects will make important targets for subsequent chemical composition studies based on high resolution spectroscopy and for confirmation of these objects with this class of identification.

While identification of C-N and C-J type stars are relatively easy, separating C-R stars from CH stars is not so straightforward. The two main properties, presence or absence of *s*-process elements and binarity that differentiate early-R stars from CH stars, can be known only through detailed abundance studies that require high resolution spectroscopy and from long-term radial velocity monitoring. The faintness of these objects makes high resolution spectroscopic studies arduous and time-consuming. As such, the method described in Goswami (2005) to distinguish a C-R from a CH star proved quite useful (Goswami et al. 2006). High resolution spectra will also allow for an accurate measurement of ¹²C/¹³C ratios. Based on medium resolution spectra, for the potential CH star candidates, we find a low (≤ 10) carbon isotopic ratios, indicating that they belong to the group of early-type CH stars.

Abia et al. (2002) have shown that CH stars cannot be formed above a threshold metallicity, around $Z \sim 0.4Z_{\odot}$. According to Dominy (1984), the metallicities of C-R stars are either solar or slightly sub-solar. C-R stars are believed to be Core Helium Burning (CHeB) counterparts of CH stars in which *s*-process elements are either absent or not detectable (Izzard et al. 2007). These authors have predicted an early-R/CH ratio $\sim 7\%$, at [Fe/H] = -2.3, a metallicity typical of the Galactic halo. This ratio is derived considering only CHeB CH stars, if CH giants and dwarfs are also considered, this ratio is likely to get much lower.

Westerlund et al. (1995) defined dwarf carbon stars as having J-H ≤ 0.75 , H-K ≥ 0.25 mag. Among the three dwarf carbon stars in our sample the objects HE 1358-2508 occupies a region defined by these limits on J-H, H-K plane. HE 0009-1824 and HE 1116-1628 however do not follow the JHK definition of dwarf carbon stars offered by Westerlund et al. (1995). It seems, these limits on J-H and H-K may not be very tight. Proper motions of these objects have been estimated by Maunon et al. (2007) and have placed them as dwarf carbon stars.

The temperature estimates of the program stars derived using JHK-temperature calibration relations of Alonso et al. (1996), although varying over a wide range, provide a preliminary temperature check for the program stars and can be used as starting values in deriving atmospheric parameters from high resolution spectra using model atmospheres.

Important information such as kinematic properties of the stars can be derived from radial velocity estimates. From

low resolution spectra, radial velocities are generally computed using Fourier cross-correlation method. This method, widely employed, uses the spectrum of a radial velocity standard as the template spectrum. Unfortunately, we could not acquire spectra of radial velocity standards that are usable for the present set of program stars under study. Estimated radial velocities using a few atomic lines, detectable on the low resolution spectra, did not return consistent results. However, a systematic estimation of radial velocities of the program stars using appropriate radial velocity standard templates would be a worthwhile future program. Radial velocities of a few stars belonging to our program star list, that are available in literature, are listed in Table 5.

The primary focus of this work is CH stars; however, a detailed discussion on the objects of other spectral types is also necessary and is under progress.

Acknowledgement

We thank the staff at IAO, VBO and at the remote control station at CREST, Hosakote for assistance during the observations. This work made use of the SIMBAD astronomical database, operated at CDS, Strasbourg, France, and the NASA ADS, USA. Ms Drisya K. is a JRF in the DST project NO. SR/S2/HEP-09/2007; funding from the above mentioned project is gratefully acknowledged.

REFERENCES

- Abia C., Dominguez I., Gallino R., Busso M., Masera S., Straniero O., de Laverny P., Plez B., Isern J., 2002, *ApJ*, 579, 817
- Alonso A., Arribas S. & Martinez-Roger C., 1994, *A&AS*, 107, 365
- Alonso A., Arribas S. & Martinez-Roger C., 1996, *A&A*, 313, 873
- Alonso A., Arribas S. & Martinez-Roger C., 1998, *A&AS*, 131, 209
- Aoki, W., Norris, J. E., Ryan, S. G., Beers, T. C. & Ando, H., 2002, *ApJ*, 567, 1166
- Aoki W., Ryan S. G., Norris J. E., Beers T. C., Ando H., & Tsangarides S., 2002, *ApJ*, 580, 1149
- Aoki, W., Beers, T.C., Christlieb, N., Norris, J.E., Ryan, S.G., & Tsangarides, S., 2007, *ApJ*, 655, 492
- Barnbaum, C., Stone, R. P. S. & Keenan, P., 1996, *ApJS*, 105, 419
- Bonifacio P., Molaro P., Beers T. C., Vladilo G., 1998, *A&A*, 332, 672
- Bothun G., Elias J. H., MacAlpine G., Mathews K., Mould J. R., Neugebauer G., Reid I. N., 1991, *AJ*, 101, No.6, 2220
- Christlieb N., Wisotzki L., Reimers D., Homeier D., Koester D., & Heber, U., 2001a, *A&A*, 366, 898
- Christlieb N., Green P. J., Wisotzki L., Reimers D., 2001b, *A&A*, 375, 366
- Cohen, J. G., Sheckman S., Thompson I., McWilliam A., Christlieb N., Melendez J., Zickgraf Franz-josef, Ramirez S., Swenson A., 2005, *ApJ*, 633, L109
- Dominy, J. F., 1984, *ApJS*, 55, 27
- Frebel, A., Christlieb, N., Norris John E., Beers Timothy C., Bessell, Michael S., Rhee Jaehon, Fechner Cora, Marsteller Brian, et al., 2006, *ApJ*, 652, 1585
- Goswami, A., Bama P., Shantikumar, N. S., Devassy Deepthi, 2007, *MNRAS*, 35, 339
- Goswami A., 2005, *MNRAS*, 359, 531
- Goswami, A., Aoki W., Beers T. C., Christlieb N., Norris J. E., Ryan S. G., Tsangarides S., 2006, *MNRAS*, 372, 343
- Green P. J., Margon B., Anderson S. F., Cook K. H., 1994, *ApJ*, 434, 319
- Green P. J. & Margon, B., 1994, *ApJ*, 423, 723
- Green, P. J., Margon, B., Anderson S. F., MacConnell D. J., 1992, *ApJ*, 400, 659
- Hartwick, F. D. A. & Cowley, A. P. 1985, *AJ*, 90, 2244
- Hill V., Barbay B., Spite M., Spite F., Cayrel R., Plez B., Beers T. C., Nordstrom B., Nissen P. E., 2000, *A&A*, 353, 557
- Izzard R. G., Jeffery C. S., Lattanzio J., 2007, *A&A*, 470, 661
- Keenan Philip C. 1993, *PASP*, 105, 905
- Lambert, D. L., Gustafsson, B., Eriksson, K., Hinkle, K. H., 1986, *ApJS*, 62, 373
- Lowrance Patrick J., Kirkpatrick J. Davy, Reid I. Neill, Cruz Kelle L., Liebert James, 2003, *ApJ*, 584, L95
- Lucatello S., Gratton R. G., Beers T. C., Carretta E., 2005, *ApJ*, 625, L833-837
- Mauron, N., Gigoyan K. S., Kendall T. R., 2007, *A&A*, 463, 969
- McClure, R. D. & Woodsworth, A. W., 1990, *ApJ*, 352, 709
- McClure, R. D., 1983, *ApJ*, 268, 264
- McClure, R. D., 1984, *ApJ*, 280, L31
- Norris, J. E., Ryan, S. G., & Beers, T. C., 1997a, *ApJ*, 488, 350
- Norris, J. E., Ryan, S. G., & Beers, T. C., 1997b, *ApJ*, 489, L169
- Norris, J. E., Ryan, S. G., Beers, T. C., Aoki, W. & Ando, H., 2002, *ApJ*, 569, L107
- Ramirez I., Melendez, J., 2004, *ApJ*, 609, 417
- Ratnatunga, K. U., 1983, PhD Thesis, Australian National Observatory
- Rossi, S., Beers, T. C. & Sneden, C. 1999, in *ASP Conf Ser.* 165, *The Third Stromlo Symposium: the Galactic Halo*, ed. B. K. Gibson, T. S. Axelrod & M. E. Putman (San Francisco: ASP), 264
- Totten, E. J., Irwin M. J., Whitelock P. A., 2000, *MNRAS*, 314, 630
- Totten, E. J. & Irwin, M. J. 1998, *MNRAS*, 294, 1
- Tsuji, T., Tomioka K., Sato H., Iye M., Okada T., et al., 1991, *A&A*, 252, L1
- Vanture, Andrew D., 1992, *AJ*, 104, 1997
- Wallerstein, G. & Knapp, G. 1998, *ARA&A*, 36, 369
- Westerlund, B. E., Azzopardi, M., Breysacher, J. Rebeirot, E., 1995, *A&A*, 303, 107
- Wisotzki, L., Christlieb N., Bade, N., Beckmann, V., Kohler T., Vanelle, C., Reimers, D., 2000, *A&A*, 358, 77
- Yamashita, Y., 1975, *PASJ*, 27, 325
- Zijlstra, A. A., 2004, *MNRAS*, 348, L23
- Zinn, R., 1985, *ApJ*, 293, 424
- Zwitter, T., Siebert A., Munari U., Freeman K. C., Siviero, A., Watson, F. G., Fullbright, J. P., Wyse, R. F. G. et al., 2008, *AJ*, 136, 421